Cretaceous Research 45 (2013) 135–154

Contents lists available at ScienceDirect

Cretaceous Research

journal homepage: www.elsevier.com/locate/CretRes

Review paper

Palynoassemblages associated with a theropod dinosaur from the Snow Hill Island Formation (lower Maastrichtian) at the Naze, James Ross Island, Antarctica

Mercedes di Pasquo [a,*], James E. Martin [b,c]

[a] Consejo de Investigaciones Cientificas y Tecnológicas (CONICET), Laboratorio de Palinoestratigrafía y Paleobotánica, CICyTTP-CONICET, Dr. Matteri y España s/n, Diamante CP E3105BWA, Entre Ríos, Argentina
[b] J.E. Martin Geoscientific Consultation, 21051 Doral Ct., Sturgis, SD 57785, USA
[c] School of Geosciences, University of Louisiana, Lafayette, LA 70504, USA

ARTICLE INFO

Article history:
Received 3 February 2013
Accepted in revised form 27 July 2013
Available online

Keywords:
Palynostratigraphy
Paleoenvironment
Snow Hill Island Formation
Early Maastrichtian
James Ross Island
Antarctica

ABSTRACT

The Cape Lamb Member of the Snow Hill Island Formation at The Naze on the northern margin of James Ross Island, east of the Antarctic Peninsula, yielded a theropod dinosaur recovered near the middle of a 90 m thick section that begins at sea level, ends below a basalt sill, and is composed of interbedded green–gray massive and laminated fine-grained sandstones and mudstones. Sixteen palynoassemblages were recovered from this section, which yielded moderately diverse assemblages with a total of 100 relatively well-preserved species. The principal terrestrial groups (32%) are represented by lycophytes (8 species), pteridophytes (15 species), gymnosperms (13 species), angiosperms (21 species) and freshwater chlorococcaleans (3 species). Marine palynomorphs (68%) belong to dinoflagellates (61 species), chlorococcaleans (6 species), and one acritarch. The vertical distribution of selected species allows the distinction of two informal assemblages, the lower *Odontochitina porifera* assemblage from the base to its disappearance in the lower part of the section, and the remaining section characterized by the *Batiacasphaera grandis* assemblage. The global stratigraphic ranges of selected palynomorphs suggest an early Maastrichtian age for this section and the entombed dinosaur that is also supported by the presence of the ammonoid *Kitchinites darwinii*. These assemblages share many species with latest Campanian–early Maastrichtian palynofloras from Vega and Humps Islands, New Zealand, and elsewhere in the Southern Ocean, establishing a good correlation among them. The dominance or frequent presence of dinoflagellates throughout the section supports the general interpretation of a shelf marine depocenter. The consistent presence of terrestrial palynomorphs suggests contributions from littoral/inland environments.

1. Introduction

The Late Cretaceous James Ross Basin (JRB) in the Antarctic Peninsula (Fig. 1) has a long history of scientific studies and today it is well known for extensive paleontological records. Determination of the age of these fossils derived from the The Naze in the JRB is a major goal of this contribution. Currently, the base of the Maastrichtian Stage in Antarctica is formally defined on the basis of a mean $^{87}Sr/^{86}Sr$ value (0.7077359) for the six best-preserved samples from a bivalve–nautiloid assemblage within the *Gunnarites antarcticus* assemblage from Cape Lamb, Vega Island (Crame et al., 1999). An absolute age of 71.0 ± 0.2 Ma was obtained for a stratigraphic level 81.5–96.5 m above the base of the *G. antarcticus* assemblage corresponding to the Campanian–Maastrichtian boundary (Crame et al., 2004). This boundary figures significantly in this contribution where the palynostratigraphic analysis of sixteen productive samples from the Cape Lamb Member of the Snow Hill Island Formation, were utilized to provide the age of a small theropod dinosaur found in this section (Case et al., 2003, 2007), located on the western side of Comb Ridge at The Naze, northern margin of James Ross Island, east of the Antarctic Peninsula (Figs. 1 and 2). Previous palynological studies from The Naze were provided by Askin (1988a), who documented a short list of palynomorphs from two samples derived from the basal López de Bertodano succession. In conjunction with other assemblages from

* Corresponding author.
E-mail addresses: medipa@cicyttp.org.ar (M. di Pasquo), JEMartinGeoscientific@gmail.com (J.E. Martin).

0195-6671/$ – see front matter © 2013 Elsevier Ltd. All rights reserved.
http://dx.doi.org/10.1016/j.cretres.2013.07.008

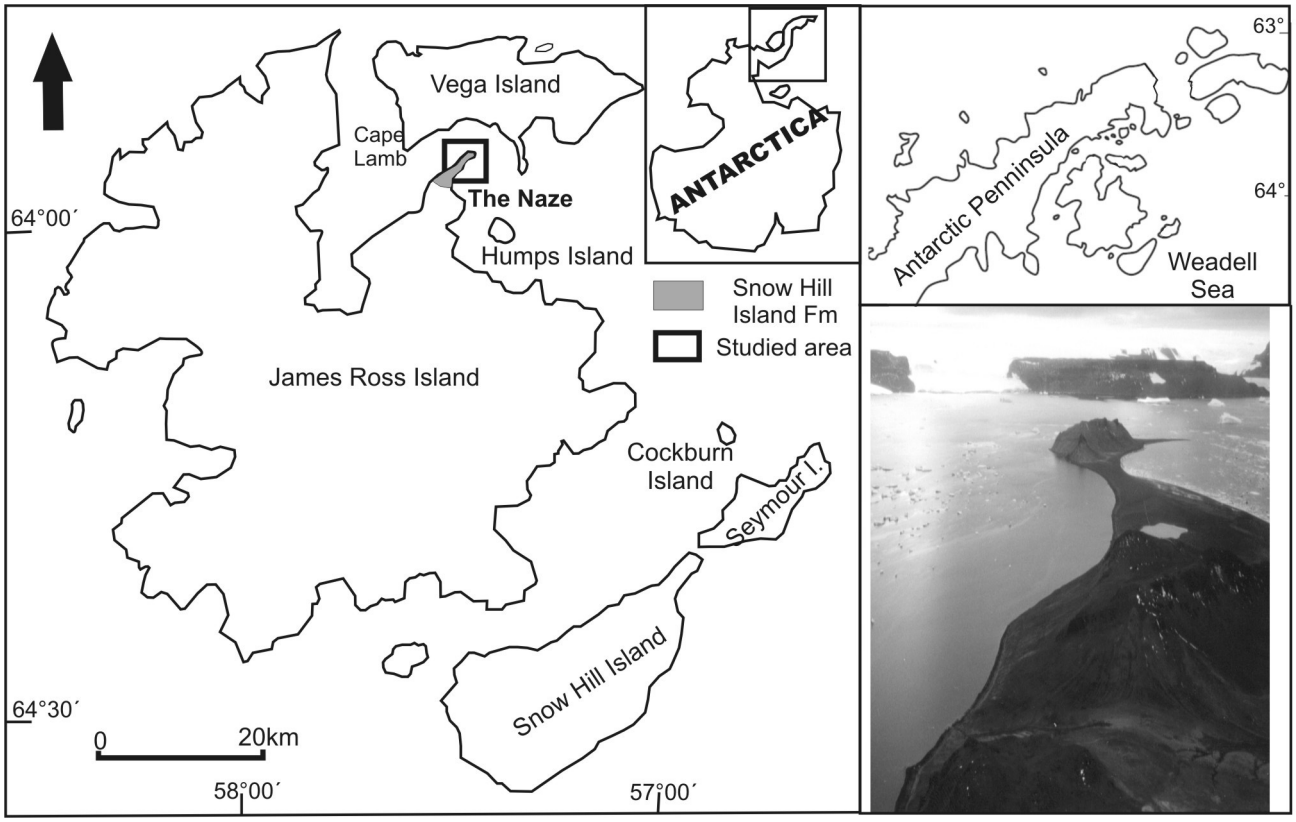

Fig. 1. Antarctic map with location of the outcrop bearing the theropod fossil remains and palynological samples here studied at the The Naze (modified from Crame et al., 2004). To the right, photograph of The Naze, a peninsula on the northern coast of James Ross Island (photo by J.E. Martin).

Vega and Seymour Islands, she proposed an informal zonation based on first appearances of several species (including *Manumiella*). Because The Naze assemblage was considered to lie below the Vega Island assemblage (Fig. 2), she considered The Naze assemblage as mid–late Campanian. This zonation from the López de Bertodano succession on Seymour Island was partially reviewed by Bowman et al. (2012) who proposed a zonation based principally on the first appearance of several species of *Manumiella* (Fig. 2). The age assignment herein for the palynoassemblages is proposed based upon the stratigraphic ranges of diagnostic palynomorph species coupled with biostratigraphic ranges of ammonoid species from The Naze section.

2. Materials and methods

The Upper Cretaceous deposits from which the Antarctic fossils (mega and micro) were collected are referred to the upper Campanian to lower Maastrichtian Cape Lamb Member of the Snow Hill Island Formation at The Naze of the James Ross Island (Figs. 1–3). As can be observed on Fig. 3, the Cape Lamb Member on the western portion of Comb Ridge (The Naze) is represented by a rather monotonous 90-m-thick section that begins at sea level and ends below a Miocene basalt sill. This Cape Lamb section is composed of interbedded green–gray massive and laminated fine-grained quartz sandstones and greenish yellow argillaceous mudstones and siltstones, interbedded with concretions and bentonite layers. The bentonites are found principally in the lower portion of the section, below the dinosaur level, but some layers occur above. The calcareous concretions are either scattered or concentrated in layers of gray claystone matrix. Interestingly, the theropod dinosaur from the middle of the section was found with several vertebrates (Martin et al., 2007; Case et al., 2003, 2007), invertebrates (ammonites, pelecypods, decapods), and palynomorphs deposited in a shelf environment. Both *Diplomoceras lambi* and *Kitchinites darwini* were found in the upper part of the section (Figs. 2 and 3). For biostratigraphical analysis, sixteen samples of argillaceous mudstones and siltstones were selected from the base and top of the section, as well as from close to significant megafossils (theropod, ammonoids, bivalves; see Fig. 3). Samples were processed using standard palynological methods (HCl, HF) at the Laboratory of Palynostratigraphy and Paleobotany (Department of Geology, Natural and Pure Sciences Faculty, University of Buenos Aires) in 2006. All were productive, and several slides were prepared with sieved residues (+25 and +10 μm) mounted with glycerin jelly. Slides and residues are housed at the Palynostratigraphy and Palaeobotany Laboratory of the CICYTTP–CONICET in Diamante (Entre Ríos, Argentina).

Identification of palynomorphs was undertaken using transmitted light microscopes and digital video camera *Nikon Eclipse* 80*i* (with DIC objectives) with a *Pax-it* (3.1 Mp) at the Laboratory of Palynostratigraphy and Paleobotany (Department of Geology, Natural and Pure Sciences Faculty, University of Buenos Aires), and a *Leica* DM500 with a fluorescence LED lamp (cold light) attached with a fluorescein (ca. 450 nm) filterblock and a 3.0 Mp videocamera (*Leica* EC3) at the CICYTTP. Different colors of the microphotographs are the result of differing equipment. A brief survey of the autofluorescence of palynomorphs was conducted, and some species of dinoflagellates and few species of spores showed light to dark orange autofluorescence. Many others did not present autofluorescence (i.e. extinguished fluorescence gray to black). The position of illustrated specimens in the respective figures, quoted with the CICYTTP-Pl acronym, are based on England–Finder coordinates.

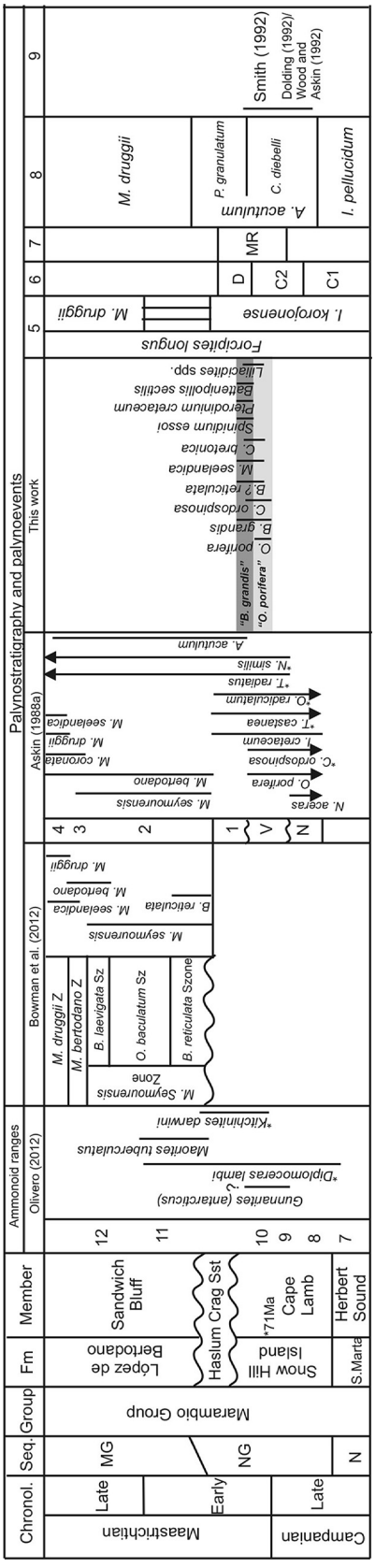

Fig. 2. Stratigraphy after Crame et al. (2004) and Olivero (2012), and absolute date after Crame et al. (1999). Sequence stratigraphy after Olivero and Medina (2000) and Olivero (2012): *Natalites* (N), Santonian–lower Campanian; *Neograhamites* and *Gunnarites* (NG), upper Campanian–lower Maastrichtian; and the *Maorites* and *Grossouvrites* (MG), lower Maastrichtian–Danian. Species of palynomorphs with an asterisk are here considered under synonymy. Species of ammonoids with an asterisk are recorded in this study. Other biostratigraphic schemes from southern Gondwana are as follows: 5-Australia (Helby et al., 1987), 6-Kerguelen Plateau (Mao and Mohr, 1992), 7-Maud Rise, Antarctica (Mohr and Mao, 1997), 8-New Zealand (Roncaglia et al., 1999), 9-James Ross Basin, Peninsula Antarctica (Vega Island: Smith, 1992, 25 species in common of 55, including the lower Maastrichtian sample D3122.3 in Dettmann and Thomson, 1987, with 40 species in common of 63; Humps Island: Dolding, 1992, 40 species in common of 140; Wood and Askin, 1992, 9 species in common of 43). Abbreviations: N-The Naze, V-Vega.

3. Geological setting

For the Upper Cretaceous James Ross Basin (JRB) in the Antarctica, Crame et al. (1991) and Crame (1992) presented a Campanian–Maastrichtian stratigraphic summary of the James Ross Island (JRI) combining stratigraphic distribution of dinoflagellates and ammonoids with that of other invertebrate fossils. The lower–upper Maastrichtian boundary was isotopically reassessed by Crame et al. (1999) based on strontium isotope dates of the base and top of the stage on Vega, Snow Hill, and Seymour Islands, James Ross Island region (northeastern Antarctic Peninsula). A comprehensive stratigraphical revision integrating lithology, biostratigraphy (e.g., ammonoids, other invertebrates, palynomorphs) and chronostratigraphy of Antarctica was presented by Crame et al. (2004). Ammonoids, in particular, were studied by several authors (see Olivero and Medina, 2000 and references therein). Olivero and Medina (2000) defined three stratigraphic sequences for the Santonian–Danian succession of the James Ross Basin; the N, Santonian–lower Campanian; the NG, upper Campanian–lower Maastrichtian; and the MG, lower Maastrichtian–Danian, sequences. The names of these sequences were derived from the most common kossmaticeratid ammonites that characterize each of them: N for *Natalites*; NG for *Neograhamites* and *Gunnarites*; and MG for *Maorites* and *Grossouvrites* (Fig. 2). Recently, Olivero (2012) addressed the sedimentary cycles, ammonite diversity, and paleoenvironmental changes in the Upper Cretaceous Marambio Group in Antarctica. He indicated that the radiation and extinction patterns in the NG and MG sequences, which are dominated by the relatively endemic kassmaticeratids, do not reflect the enlargement and reduction of the shelf during transgressions and regressions.

Other paleontological records include wood fossils (e.g., Francis, 1986, 1991) and paleovertebrates, especially marine reptiles (e.g., disarticulated plesiosaur and mosasaur skeletons, sharks teeth and vertebrae) were also recorded and studied from several places in the JRB (Martin et al., 2002, 2007; Martin and Crame, 2006; Case et al., 2007, and their references). Several palynological studies were also carried out in this basin by Baldoni (1992), Baldoni and Barreda (1986), Dettmann (1986), Dettmann and Thomson (1987), Baldoni and Medina (1989), Askin (1988a, 1988b, 1990a, 1990b, 1994, 1999), Pirrie et al. (1991, 1997), Riding et al. (1992), Smith (1992), Dolding (1992), Wood and Askin (1992), Thorn et al. (2009), Bowman et al. (2012). Some studies were conducted in different areas on James Ross Island (and closer islands) and were published together in 1992 (e.g., Pirrie et al., 1992). Of these studies, those of Smith (1992) from Cape Lamb on Vega Island and Dolding (1992) from Humps Island compared most favorably (Fig. 2) with those analyzed herein.

4. Palynological results

The marine and terrestrial assemblages recovered from the Cape Lamb Member are diverse with numerous specimens per sample level and fairly well-preserved with minimal thermal maturation. The overall composition of the assemblage (sixteen sample levels), is represented by spores (5.3%), pollen grains (18%), chlorophytes (8.7%), dinoflagellates and acritarch (66.6%), and remaining groups (2%). The principal terrestrial groups (32%) are represented by lycophytes (8 species), pteridophytes (15 species), gymnosperms (13 species), angiosperms (21 species) and freshwater chlorococcaleans (3 species). Marine palynomorphs (68%) belong to dinoflagellates (61 species), chlorococcaleans (6 species), and one acritarch. Complementary groups such as bryophytes, sphenophytes, organic foraminiferal linings, microthyriaceae fungi and copepod eggs are also intermittently present (Figs. 3 and 4).

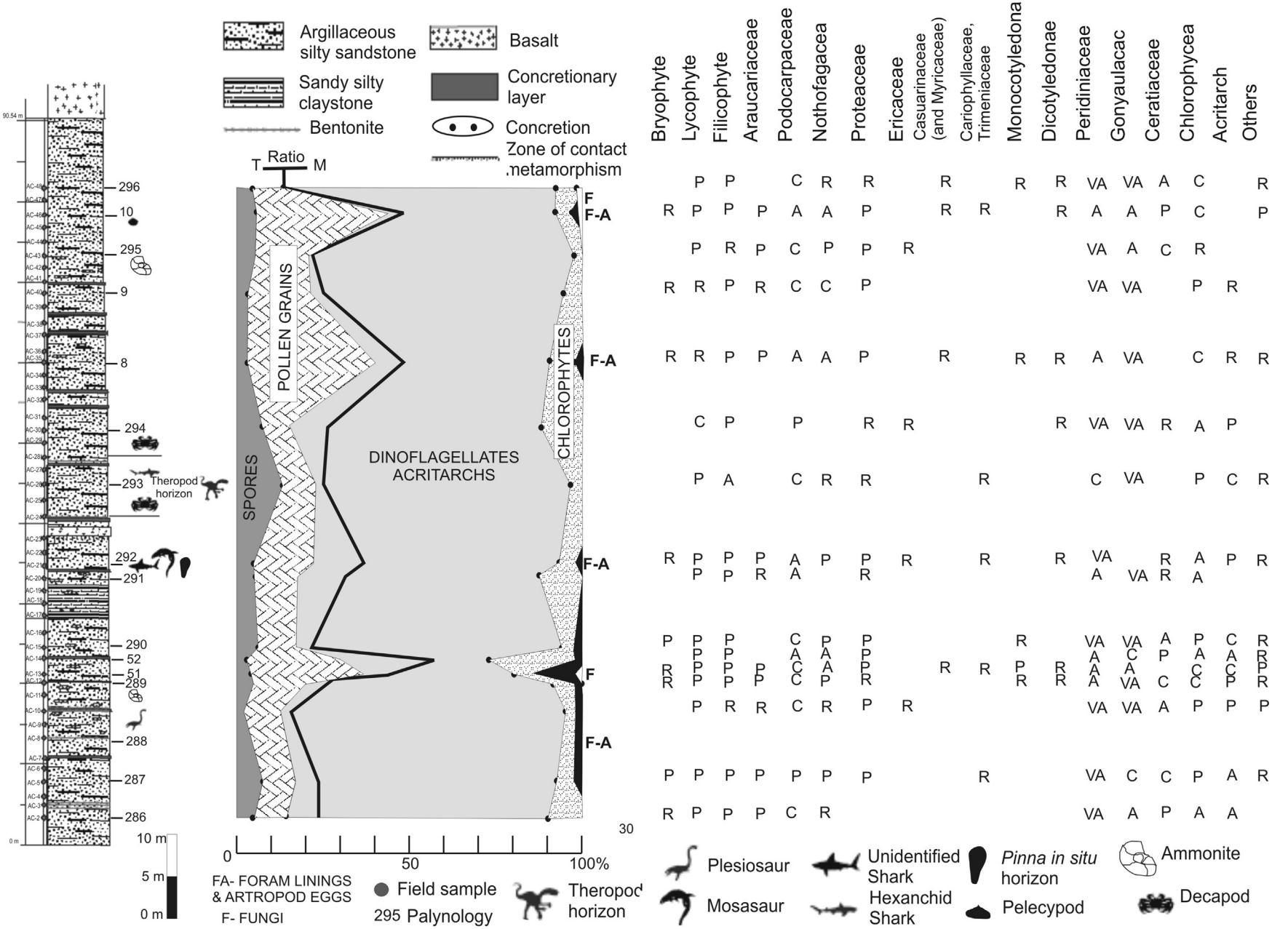

Fig. 3. Stratigraphic section at The Naze showing quantitative occurrences of main groups of palynomorphs after their biological affinities and in stratigraphical order. The database is presented in Fig. 4. Their relative frequencies (based on counts of 250 to 400 specimens per sample) are represented as follows: R-rare (<1%), P-Present (<5%), C-Common (<10%), A-Abundant (10–30%) and **VA**- (>30–60%, considered as a "bloom" or peak of abundance). Location of other fossils is also depicted. T–M-Terrestrial:Marine Ratio.

Semi-quantitative stratigraphic distribution of selected palynomorphs along the section is provided in Fig. 5. The complete list of taxa (with full authority) documented at The Naze is presented in Fig. 4, ordered by major groups and following a stratigraphical order. Illustrations of selected species (Figs. 7–11) are in the Appendix A.

The database of Raine et al. (2011) was used to classify most of the terrestrial palynomorphs along with their botanical affinities, whereas dinoflagellates and algal identification were chiefly based on the Dinoflaj Database (Fensome et al., 2008), although later taxonomical contributions were also used (e.g., Thorn et al., 2009; Sluijs et al., 2009). Taxonomical remarks are addressed in the list of taxa, along with synonymies of several species illustrated, especially by Askin (1988a), among other authors (see Fig. 2 and Chart 1, supplementary online material). All synonymies were carefully based on identical morphologies; hence ancillary remarks are included only when deemed necessary. The known global stratigraphic ranges of selected palynomorphs are depicted in Fig. 6 based on information provided in Chart 1 (Supplementary online information).

A

SPECIES / Repository number (CICYTTP-PI)		286	287	288	289	51	52	290	291	292	293	294	8	9	295	10	296
AB	Spores / field sample number	AC-2	AC-5	AC-10	AC-12-1	AC-13	AC-14	AC-15	AC-20	AC-21	AC-26	AC-30	AC-35	AC-40	AC-43	AC-46	AC-48
LY	*Perotrilites majus* (Cookson and Dettmann 1958) Evans 1970	1,90%	1,71%	0,53%	0,92%			1,65%	1,32%	0,85%		1,51%			1,65%	0,29%	1,28%
LY	*Retitriletes austroclavatidites* (Cookson 1953) Doring et al. in Krutzsch 1963	0,95%	1,37%	1,06%	0,92%	1,89%	1,91%	1,65%	2,19%	1,41%	1,33%	3,52%	0,89%	0,38%	1,65%	2,00%	0,85%
F	*Baculatisporites comaumensis* (Cookson 1953) Potonié 1956	0,24%	0,34%	0,27%	0,69%	1,26%	0,27%	0,55%	1,32%	0,28%		1,01%	0,30%	1,53%	0,83%		1,28%
F	*Cyathidites australis /C. minor* Couper 1953	0,24%	0,34%	0,27%	0,69%	0,32%	0,55%		0,44%	0,85%			0,59%			0,86%	
F	*Birretisporites potoniaei* Delcourt and Sprumont 1955	0,24%				0,32%										0,29%	
F	*Todisporites major /T. minor* Couper 1958	0,24%			0,69%		0,27%	0,55%			1,33%		0,59%			0,29%	0,43%
LY	*Ceratosporites equalis* Cookson and Dettmann 1958	0,47%			0,46%					1,13%							
B	*Triporoletes radiatus* (Dettmann 1963) Playford 1971	0,47%	2,74%		0,23%			1,10%		0,28%						0,29%	
F	*Laevigatosporites ovatus* Wilson and Webster 1946/*L. major* (Cookson) Krutzsch 1959		0,34%			0,32%	0,55%					0,50%	0,89%	0,38%		0,29%	
B	*Stereisporites antiquasporites* (Wilson and Webster) Dettmann 1963		0,34%										0,30%				
F	*Ischyosporites volkheimeri* Filatoff 1975			0,27%				0,55%		0,28%							0,43%
LY	*Herkosporites* sp.				0,23%												
F	*Polypodiisporites* sp.				0,23%												
LY	*Densoisporites velatus* Weyland and Krieger 1953				0,23%									0,38%			
B	*Stereisporites regium* (Drozhastichich) Drugg 1967					0,63%							0,30%	0,38%		0,57%	
F	*Gleicheniidites senonicus* Ross 1949 (=*Gleichenidites circinidites* (Cookson) Brenner)					0,32%											0,43%
F	*Cyatheacidites annulatus* Cookson 1947							0,55%			3,33%						
LY	*Lycopodiumsporites eminulus* Dettmann 1963								0,44%						0,83%		
LY	*Camarozonosporites ohaiensis* (Couper 1953) Dettmann and Playford 1968									0,28%							
S	*Calamospora* sp.										0,67%						
F	*Trilites parvallatus* Krutzsch 1959										0,67%						
F	*Cyatheacidites archangelskii* Dettmann 1986										6,00%	1,01%					
LY	*Dictyotosporites speciosus* Cookson and Dettmann 1958											0,50%					
F	*Tuberculatosporites parvus* Archangelsky 1972											0,50%					
F	*Polypodiisporites favus* (Potonié) Potonié 1934													0,38%			
F	*Peromonolites bowenii* Couper 1953													0,38%		0,29%	
F	cf. *Klukisporites scaberis* (Cookson and Dettmann 1958) Dettmann 1963															0,29%	
	Gymnosperm pollen grains																
A	*Araucariacites australis* Cookson 1947	0,47%	0,68%		1,61%	1,26%			0,44%	1,69%			0,59%	0,38%	1,65%	1,43%	
P	*Phyllocladidites mawsonii* Cookson 1947 ex Couper 1953	0,71%	1,37%	1,06%	2,30%	1,26%	2,46%	1,65%	1,32%	1,13%	0,67%		4,73%	3,44%	0,83%	4,00%	0,43%
P	*Podocarpidites rugulatus* Pocknall and Mildenhall 1984	0,47%	0,68%		0,23%	1,58%	3,01%		1,32%		0,67%	0,50%	0,30%	0,76%		1,14%	0,85%
P	*Podocarpidites* spp.	4,03%	2,40%	5,31%	4,61%	0,32%	3,83%	5,49%	4,39%	12,96%	3,33%	3,02%	1,78%	4,58%	6,61%	7,43%	2,13%
A	*Dilwynites granulatus* Harris 1965	0,95%	0,34%	0,80%	0,46%	0,63%							1,18%			2,29%	
P	*Podocarpidites marwickii* Couper 1953	0,24%	0,34%			0,95%	0,27%		0,88%				0,59%			0,29%	0,85%
P	*Podocarpidites major* Couper 1953	0,24%			0,23%	0,32%											
P	*Trichotomosulcites subgranulatus* Couper 1953	0,24%					1,09%			0,28%			4,14%	1,15%	1,65%	0,57%	0,43%
P	*Podocarpidites otagoensis* Couper 1953			0,53%		0,63%				0,28%	0,67%	0,50%	0,59%				0,43%
P	*Microcachrydites antarcticus* Cookson 1947 ex Couper 1953			0,53%	0,23%	0,95%	0,82%		2,63%	0,28%	0,67%		0,30%			1,14%	
P	*Dacrycarpites australiensis* Cookson and Pike 1953			0,27%					0,88%	0,56%	0,67%						
E	*Equisetosporites* sp.					0,95%											
P	*Podocarpidites verrucosus* Volkheimer 1972															0,57%	
	Angiosperm pollen grains																
N	*Nothofagidites dorotensis* Romero 1973	0,24%								0,28%			0,30%				0,43%
N	*Nothofagidites* spp	0,71%	3,42%	0,27%	1,84%	13,88%	11,20%	1,10%		0,28%	0,67%		16,27%	5,73%	1,65%	12,00%	
Pr	*Peninsulapollis gillii* (Cookson 1957) Dettmann and Jarzen 1988		0,34%	0,53%	0,46%	2,52%	1,91%	1,65%	0,44%	1,13%	0,67%	0,50%	1,48%		1,65%	3,43%	0,85%
Pr	*Peninsulapollis askiniae* Dettmann and Jarzen 1988		0,34%	0,53%	0,46%	0,32%							0,59%			0,29%	
C-T	*Periporopollenites polyoratus* (Couper 1960) Stover in Stover and Partridge 1973		0,34%			0,32%				0,28%	0,67%					0,29%	
Pr	*Proteacidites* spp.		0,34%				1,37%						1,18%	0,38%			
Er	*Ericipites scabratus* Harris 1965			0,27%						0,28%		1,01%			0,83%		
Pr	*Proteacidites tenuiexinus* Stover in Stover and Partridge 1973			0,27%			0,27%										
M-L	*Liliacidites* spp.				0,92%	1,26%		0,55%					0,59%				
N	*Nothofagidites americanus* Zamaloa 1992				0,46%	0,63%				0,56%			0,59%				
D	*Triorites orbiculatus* McIntyre 1965				0,23%										0,83%	0,29%	
M	*Monosulcites palisadus* Couper 1953					0,63%											
M	*Monosulcites/Arecipites* spp.					1,58%											
N	*Nothofagidites tehuelchesii* Zamaloa and Barreda 1992					0,32%											
D	*Tricolpites confessus* Stover in Stover and Partridge 1973					0,32%				0,28%		1,01%	0,30%				
C-M	*Myricipites harrisii* (Couper 1953) Dutta and Sah 1970 (=*Haloragacidites trioratus* Couper 1953					0,63%							0,30%			0,29%	0,43%
D	*Battenipollis sectilis* (Stover) Jarzen and Dettmann 1991									0,28%						0,29%	
N	*Nothofagidites saraensis* Menéndez and Caccavari de Filice 1975												0,30%				
Pr	*Proteacidites scaboratus* Couper 1960													0,38%			
Pr	*Proteacidites parvus* Cookson 1950													0,38%		0,86%	
M-L	*Longapertites* sp. in Povilauskas et al. 2008																0,85%

Fig. 4. Percentages and stratigraphic distribution of taxa documented along the Comb Range section at The Naze. Biological affinities are also included in the row on the left. Abbreviations: B-Bryophyte, LY-Lycophyte, S-Sphenophyte, F-Filicophyte–Pterophyte (Fern), A-Araucariaceae, P-Podocarpaceae, E-Ephedraceae, N-Nothofagaceae, Pr-Proteaceae, Er-Ericaceae, C–M-Casuarinaceae, possibly also Myricaceae, C–T-Caryophyllaceae, Trimeniaceae, M-Monocotyledonae, M–L-Monocotyledonae, D-Dicotyledonae, Per-Peridiniaceae, Gon-Gonyaulacaceae, Cer-Ceratiacea, Clo-Chlorophyceae, Ac-Acritarch, Mf-Linings of forams, Fg-Fungi – Microthyriaceae (*Asterothyrites* Cookson), Co-Copepods eggs.

B

	Chlorophyceae																
Clo	*Botryococcus brauni* Kützing 1849	4,74%	2,05%	0,80%	2,07%	3,15%	4,64%		2,19%	3,94%		5,03%	5,92%	1,15%		4,29%	2,55%
Clo	*Nummus monoculatus* Morgan 1975	3,08%	2,05%	0,27%	1,61%	2,21%	0,27%	2,75%	3,07%	3,66%	1,33%	1,51%	1,78%	1,15%		1,14%	2,13%
Clo	*Palambages* spp.	1,42%	0,34%	0,80%	0,92%		0,55%	1,10%	3,07%	0,56%	0,67%	1,51%	0,30%			1,14%	
Clo	*Leiosphaeridia* sp.	0,47%			3,00%	0,63%	20,49%		2,63%	2,82%		2,01%	0,59%	0,76%			1,28%
Clo	*Tetraedron* cf. *minimum* (A. Braun) Hansgirg 1988					0,32%								0,38%			0,43%
Clo	*Pterospermella* spp.						0,27%						0,30%				
Clo	*Dictyotidium* sp.						0,82%						0,59%				
Clo	*Paralecaniella indentata* (Deflandre and Cookson) Cookson and Eisenack 1970 emend Elsik 1977	0,24%	0,34%	0,53%					1,32%	0,28%	0,67%	1,51%		0,76%	0,83%		1,28%
Clo	*Pterospermella autraliensis* (Deflandre and Cookson) Eisenack 1972								0,44%								
	Acritarchs																
Ac	*Michrystridium piliferum* Deflandre 1937	14,22%	27,40%	1,86%	1,84%	5,36%	12,30%	5,49%		4,23%	6,67%	5,03%	0,89%	0,76%			
Mf	Linnings of forams			0,80%		0,63%	0,55%	0,55%		0,28%			0,89%			1,14%	
Fg	Fungi – Microthyriacea: *Asterothyrites* Cookson 1947				0,23%											0,29%	0,85%
Co	Copepods eggs		0,68%	0,27%	0,46%	11,04%											
	Dinoflagellate																
Per	*Chatangiella victoriensis* (Cookson and Manum) Lentin and Williams 1977	1,42%	0,68%														
Gon	*Cyclonephelium compactum* Deflandre and Cookson 1955	0,47%															
Per	*Diconodinium* sp. cf. *multispinum* (Deflandre and Cookson) Eisenak and Cookson emend Morgan 1977	0,24%		0,27%								0,50%					
Gon	*Operculodinium flucturum* Davey 1969	1,90%															
Per	*Xenikoon australis* Cookson and Eisenack 1960	0,95%								0,56%							
Per	*Amphidiadema nucula* (Cookson and Eisenack) Lentin and Williams 1976	1,66%	1,37%	0,80%	1,84%					0,56%				1,15%		2,00%	2,13%
Gon	*Valensiella reticulata* (Davey) Courtinat 1989	0,24%								0,28%							
Gon	*Trichodinium castanea* (Deflandre) Clarke and Verdier 1967 - *T. chilensis* Troncoso and Doubinger 1980	0,24%		0,27%	1,15%	15,77%	0,27%	4,40%	21,93%	1,41%	40,00%	4,02%	11,24%	17,18%	4,96%	4,57%	8,51%
Cer	*Odontochitina porifera* Cookson 1956	1,90%	4,11%	1,86%	1,84%												
Per	*Andalusiella mauthei* Riegel 1974	0,24%			0,23%			0,55%	1,75%	0,28%							
Per	*Manumiella druggii* (Stover 1974) Bujak and Davies 1983	0,24%										1,01%					
Per	*Manumiella seymourensis* Askin 1999	0,95%	1,03%	1,06%	1,61%			0,55%					0,30%		5,79%	0,57%	
Per	*Maduradinium pentagonum* Cookson and Eisenack 1970	0,24%	0,68%	1,06%	1,15%	0,32%		0,55%	0,88%	0,56%		1,01%		0,76%	1,65%		1,28%
Per	*Manumiella* spp.	0,24%	1,03%							0,85%			0,30%				
Gon	*Batiacasphaera grandis* Roncaglia et al. 1999	1,66%	1,37%	2,39%	0,92%	0,32%	0,27%	1,65%	2,19%	1,69%	1,33%	7,54%	2,96%	8,02%	3,31%	2,00%	4,26%
Gon	*Canningia* sp. 1 in Schioler and Wilson 1998	4,27%	0,34%	0,53%	1,84%			7,69%		1,13%		2,01%					0,43%
Per	*Chatangiella granulifera/verrucosa* (Manum 1963) Lentin and Williams 1976	7,11%	6,85%						0,44%								
Per	*Isabelidinium cretaceum* (Cookson 1956) Lentin and Williams 1977	11,85%	7,88%	18,57%	12,67%	16,72%	15,30%	5,49%	1,75%	14,93%	2,00%	5,03%	12,72%	16,79%	12,40%	15,43%	4,26%
Per	*I. cretaceum gravidum* Mao and Mohr 1992	2,37%	3,77%	2,65%	2,07%	0,32%	0,27%	5,49%	1,75%	1,97%	2,00%	5,03%	0,89%		8,26%		4,26%
Per	*Isabelidinium pellucidum* (Deflandre and Cookson 1955) Lentin and Williams 1977	4,74%	0,34%	1,59%	0,92%	0,63%	0,27%	2,20%		1,13%	0,67%		0,59%	0,76%	1,65%	0,57%	2,13%
Gon	*Spongodinium reticulatus* Hultberg 1985	0,24%	0,34%	0,27%	0,92%	0,32%			0,88%	0,56%		5,03%	0,30%			0,29%	1,28%
Per	*Nelsoniella aceras* Cookson and Eisenack 1960	0,71%	0,68%	0,27%	0,23%	0,32%	0,27%	1,65%		0,28%		0,50%			1,65%		
Gon	*Operculodinium radiculatum* Smith 1992	10,66%	2,05%	2,65%	7,60%	1,89%	2,73%	2,75%	2,63%	3,38%	13,33%	5,03%	9,76%	2,29%	4,13%	4,86%	8,51%
Per	*Isabellidinium* sp.		1,03%	1,59%	0,92%	0,32%	0,55%	5,49%	2,63%		1,33%	3,02%	0,59%		4,13%	0,57%	4,26%
Per	*Palaeocystodinium granulatum* (Wilson 1967) Lentin and Williams 1976	0,24%	0,68%	0,27%					0,88%			0,50%					
Gon	*S. ramosus (ramosus-multibrevis-granosus)* complex (*Spiniferites ramosus* (Ehrenberg 1838) Mantell 1854	4,74%	4,45%	21,22%	12,21%	1,58%	3,01%	10,99%	13,16%	9,86%	2,00%	7,54%	4,73%	7,25%	4,96%	6,29%	8,51%
Cer	*Xenascus plotei* Below 1981	0,47%	0,68%	14,59%	6,22%		4,92%	10,99%	3,51%	2,25%		1,51%			4,13%	3,43%	8,51%
Per	*Paleocystodinium pilosum* Guler et al. 2005	0,47%	0,34%	1,86%	1,84%		0,27%			0,28%	0,67%	2,51%	0,89%	8,78%	3,31%	2,57%	1,28%
Per	*Saeptodinium gravattensis* Harris 1973	1,18%		0,27%	1,38%		0,27%		1,75%				0,30%	0,38%			1,70%
Per	*Eurydinium ellipticum* Mao and Mohr 1992	0,71%			0,46%												2,55%
Per	*Canninginopsis ordospinosa* Smith 1992	0,24%	6,85%	1,06%		0,32%	1,37%	3,30%	4,39%	3,94%							
Gon	*Impagidinium cristatum* (May) Lentin and Williams 1981	0,24%		0,27%				0,55%		0,28%		0,50%	0,30%		0,83%		0,43%
Cer	*Odontochitina indigena* Marshall 1988		0,34%														0,43%
Per	*Isabellidinium cretaceum oviforme* Mao and Mohr 1992		1,71%		1,38%	0,32%	0,55%	2,75%		1,69%		3,52%			4,13%	2,29%	4,26%
Gon	*Batiacasphaera? reticulata* (Davey) Davey 1979		0,34%			0,32%		1,65%	2,19%	0,56%	2,67%	2,51%	0,59%	0,76%	1,65%	0,29%	1,28%
Per	*Phelodinium exilicornutum* Smith 1992		0,34%		0,23%			1,65%	1,75%	0,56%	1,33%	2,01%	0,30%		4,13%		1,28%
Gon	*Membranilarnacia* spp.			0,27%	0,23%									0,38%			0,43%
Per	*Isabellidinium papillum* Sumner 1992			0,27%		0,32%											0,85%
Per	*Alterbidinium acutulum* (Wilson) Lentin and Williams 1976			0,27%				0,55%		0,28%							
Per	*Canninginopsis bretonica* Marshall 1990			0,53%					1,32%	1,13%							
Gon	*Operculodinium centrocarpum* (Deflandre and Cookson) Wall 1967			4,51%	8,06%					4,79%		0,50%	0,59%		0,83%	1,71%	1,28%
Per	*Paleocystodinium golzowense* Alberti 1961			0,53%										2,29%		0,57%	0,85%
Gon	*Batiacasphaera rifensis* Slimani et al. 2008			0,27%						0,56%					0,83%		
Per	*Manumiella conorata* (Stover) Bujak and Davies 1983				0,46%				0,88%			3,02%		0,76%			
Per	*Manumiella seelandica* (Lange) Bujak and Davies 1983				0,23%	0,32%		0,55%			0,67%		0,30%	5,73%		0,29%	
Gon	*Kallosphaeridium? ringnesorium* in Mohr and Mao 1997				1,15%												
Cer	*Xenascus ceratioides* (Deflandre) Davey and Verdier 1971				0,69%					0,85%					1,65%	1,14%	2,13%
Gon	*Circulodinium distinctum* (Deflandre and Cookson) Jansonius 1986					0,32%							0,89%	0,76%		0,57%	
Gon	*Batiacasphaera rugulata* Schioler and Wilson 1998							1,65%		0,28%		1,51%					0,43%
Per	*Spinidium essoi* Cookson and Eisenack 1967								0,88%	0,28%							
Gon	*Spiniferites pseudofurcatus* (Klump) Sarjeant 1970								1,32%								0,43%
Per	*Diconodinium cristatum* Cookson and Eisenack 1974 emend Morgan 1977								0,44%								
Per	*Cerodinium* sp. in Mehrotra and Sarjeant 1987									0,28%							
Gon	*Kallosphaeridium parvum* Jan du Chêne 1988									0,56%							
Per	Indeterminate Dinoflagellate									0,28%							
Gon	*Pterodinium cretaceum* Slimani et al. 2008										0,67%						0,43%
Per	*Isabellidinium cooksoniae* (Alberti) Lentin and Williams 1977											0,50%					
Per	*Manumiella* sp. cf. *M. bertodano* Thorn et al. 2009											2,01%	0,30%		4,13%		
Per	*Senegalinium bicavatum* Jain and Millepied 1973											0,50%					
Per	*Nelsoniella tuberculata* Cookson and Eisenack 1960																0,85%
	Number of specimens counted	**422**	**292**	**377**	**434**	**317**	**366**	**182**	**228**	**355**	**150**	**199**	**338**	**262**	**121**	**350**	**235**
	SPECIES / Repository number (CICYTTP-PI)	**286**	**287**	**288**	**289**	**51**	**52**	**290**	**291**	**292**	**293**	**294**	**8**	**9**	**295**	**10**	**296**

Fig. 4. (*continued*).

STAGE	INFORMAL ASSEMBLAGES	FIELD SAMPLE	LAB CICYTTP-PI	TERRESTRIAL SP.						MARINE SPECIES																															
				Triporoletes radiatus	*Cyatheacidites* spp.	*Penninsulapollis* spp.	*Periporopollenites polyoratus*	*Ericipites scabratus*	*Battenipollis sectilis*	*Trichodinium castaneum- chilensis*	***Odontochitina porifera***	*Manumiella druggii*	*Manumiella seymourensis*	***Batiacasphaera grandis***	*Canningia* sp. 1 Schioler and Wilson	*Chatangiella granulifera*	*Isabellidinium cretaceum cretaceum*	*Isabellidinium cretaceum gravidum*	*Isabellidinium pellucidum*	*Spongodinium reticulatum*	*Operculodinium radiculatum*	*Paleocyst. granulatum-golzowense*	*Spiniferites ramosus* complex	*Xenascus plotei*	*Paleocystodinium pilosum*	*Saeptodinium gravattensis*	*Eurydinium ellipticum*	*Canninginopsis ordospinosa*	*Impagidinium cristatum*	*Batiacasphaera? reticulata*	*Phelodinium exilicornutum*	*Alterbidinium acutulum*	*Canninginopsis bretonica*	*Batiacasphaera rifensis*	*Manumiella coronata*	*Manumiella seelandica*	*Spinidium essoi*	*Pterodinium cretaceum*	*Senegalinium bicavatum*	*Nummus monoculatus*	*Michrystridium piliferum*
Early Maastrichtian	***Batiacasphaera grandis***	AC-48	296			R				C				P	R		P	P	P	P	C	R	C	C	P	P	P		R	P	P							R		P	
		AC-46	10	R		P	R		R	P			R	P			A		R	R	P	R	C	P	P					R						R				P	
		AC-43	295			P		R		P			C	P			A	C	P		P		P	P	P				R	P	P			R							
		AC-40	9							A				C			A		R		P	P	C		C	R				R					R	P				P	R
		AC-35	8			P				A			R	P			A	R	R	R	C		P		R	R			R	R	R					R				P	R
		AC-30	294		P	R		P		P		P		C	P		C	C		C	C	R	C	P	P				R	P	P				P				R	P	C
		AC-26	293		C	R	R			VA				P			P	P	R		A		P		R					P	P					R		R		P	C
		AC-21	292	R		P	R	R	R	P				P	P		A	P	P	R	P		C	P	R			P	R	R	P	R	P	R			P			P	P
		AC-20	291			R				A				P		R	P	P		R	P	R	A	P		P		P		P	P		P		R		R			P	
		AC-15	290	P	R	P				P			R	P	C		C	C	P		P		A	A				P	P	P	P	R				R				P	C
		AC-14	52			P				R				R			A	R	R		P		P	P	R	R		P												R	A
		AC-13	51			P	R			A				R			A	R	R	R	P		P					R		R						R				P	C
	O. porifera	AC-12	289	R		R				P	P		P	R	P		A	P	R	R	C		A	C	P	P	R				R				R	R				P	P
		AC-10	288			P		R		R	P		P	P	R		A	P	P	R	P	R	A	A	P			P	R			R	R	R						R	P
		AC-5	287	P		R	R				P		P	P	R	P	C	P	R	R	P	R	P	R	R	R		C		R	R									P	A
		AC-2	286	R						R	P	R	R	P	P	C	A	P	P	R	A	R	P	R	R	P	R	P	R											P	A

Fig. 5. Relative frequencies (based on counts of 250–400 specimens per sample) of selected taxa along the section are represented as follows: R-rare (<1%), P-Present (<5%), C-Common (<10%), A-Abundant (10–30%) and **VA**- (>30–60%, considered as a “bloom” or peak of abundance). The database is presented in Fig. 4.

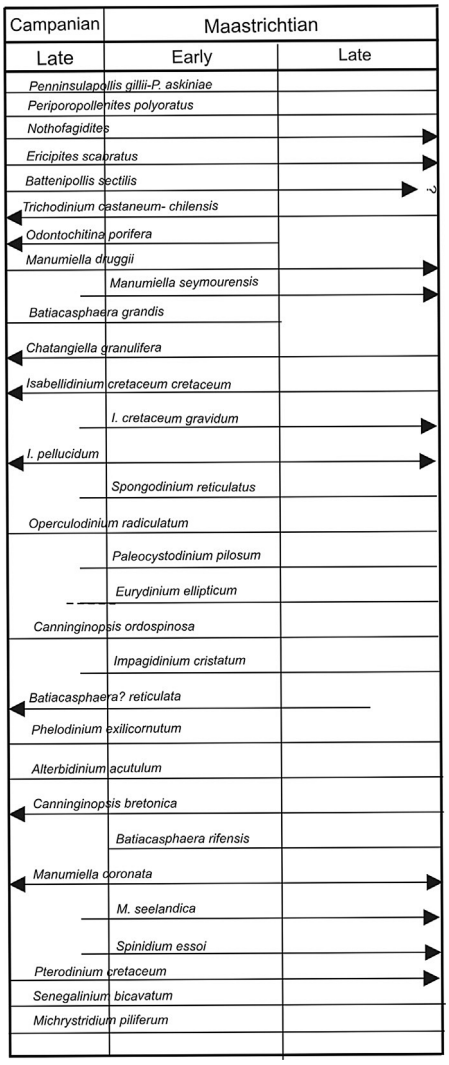

Fig. 6. Global stratigraphic range of selected species recorded at The Naze section (based on information provided in Chart 1 of the supplementary online information).

Spores

Biretisporites potoniaei Delcourt and Sprumont 1955 (Fig. 7C)
Birretisporites sp. Barreda et al., 1999; Pl. 1, fig. 1.
Birretisporites sp. A Dettmann and Thomson, 1987; Fig. 3, b.

Camarozonosporites ohioensis (Couper) Dettmann and Playford 1968
Camarozonosporites ambigens (Fradkina) Playford, 1971 (auct. non); Barreda et al. (1999), Pl. 1, Fig. 7.

Triporoletes radiatus (Dettmann) Playford 1971 (Fig. 7N)
Gen and sp. Askin, 1988a, Fig. 8.10.
Gen and sp. Askin, 1988a, Smith (1992), Fig. 11, m–p.
Gen and sp. Askin, 1988a, Dolding (1992), Fig. 6, n.

Pollen

Gymnosperm

Podocarpidites otagoensis Couper 1953 (Fig. 7M)
Podocarpidites elegans Romero, 1977; Pl. 3, Figs. 1–11.

Dinoflagellate

Batiacasphaera grandis Roncaglia et al. 1999 (Fig. 10K, L)
Canningia? sp.1 Ioannides and McIntyre, 1980; Pl. 31.2, Fig. 1, 3.

Batiacasphaera rifensis Slimani et al. 2008 (Fig. 9A)
Batiacasphaera cf. *kekerengensis* Marenssi et al., 2004; Fig. 5N, O.

Batiacasphaera? reticulata (Davey) Davey 1979 (Fig. 9C, D)
Batiacasphaera sp. Pirrie et al., 1997; Fig. 10i.

Canninginopsis ordospinosa Smith 1992 (Fig. 9BB)
cf. *Canninginopsis* sp. Askin, 1988a; Fig. 7.6.

Impagidinium cristatum (May) Lentin and Williams 1981 (Fig. 10E, F)
Pterodinium sp. Schiøler and Wilson, 1998; Pl. 6, Fig. 8.

Isabelidinium cretaceum gravidum Mao and Mohr 1992 (Fig. 9B)
Isabellidinium cf. *bakeri* Smith, 1992; Fig. 7f.

Odontochitina indigena Marshall 1988 (Fig. 10O)
Xenascus sp. Wood and Askin, 1992; Fig. 5d.

Operculodinium radiculatum Smith 1992 (Fig. 11F)
Operculodinium sp. Askin, 1988a; Fig. 7.7.
Operculodinium sp. Wood and Askin, 1992; Fig. 4e.

Phelodinium exilicornutum Smith 1992 (Fig. 9U)
Octodinium askiniae Wrenn and Hart 1988 (auct. non), Wood and Askin, 1992; Fig. 4j.
Phelodinium sp. Askin, 1988a; Fig. 7.8.

Spongodinium reticulatum Hultberg 1985 (Fig. 10B)
Cyclonephelium cf. *clathromarginatum* Smith, 1992; Fig. 8d.
Leberidocysta sp. A Mohr and Mao, 1997; Pl. 1, Figs. 10, 14.

Trichodinium castaneum (Deflandre) Clarke and Verdier 1967 – *T. chilensis* Troncoso and Doubinger 1980, plexus (Fig. 10M, P, Q)
Cribroperidinium sp. Askin, 1988a; Fig. 7.4.
Cribroperidinium sp. A Dettmann and Thomson, 1987; Fig. 8b.
Cribroperidinium muderongense (Cookson and Eisenack) Davey 1969 (auct. non), Wrenn and Hart, 1988; Fig. 18, 1.
Cribroperidinium edwarsii (Cookson and Eisenack) Davey 1969 (auct. non), Wrenn and Hart, 1988, Fig. 18, 3–4.
Remarks: Specimens attributable to *Trichodinium castanea* associated with those of *Trichodinium chilensis* (from the upper Maastrichtian of southern Chile) in the same levels supports our proposal of a taxonomic group (plexus) among these species. T. *chilensis* is distinguished from *T. castanea* mainly in having a less spheroidal cyst with a longer apical horn and a more prominent and dense ornamentation of spines overall except for the equatorial cingulum where the spines are shorter. Askin (1988a, Fig. 7, 4) illustrated *Cribroperidinium* sp. from Zone 1 at The Naze on JRI and Cape Lamb on Vega Island that she considered equivalent to *Cribroperidinium* sp. A Dettmann and Thomson (1987, Fig. 8b). The specimens illustrated by Wrenn and Hart (1988) as *Cribroperidinium muderongense* (Fig. 18, 1) and *C. edwarsii* (Fig. 18, 3–4), considered reworked from the Cretaceous in the Paleogene of JRI in Antarctica, and are so similar to this group that they are here reassigned to this complex.

Xenascus plotei Below 1981 (Fig. 11H, J)
Xenascus sp. Barreda et al. 1999; Pl. 6, Fig. 13.

Chlorophyceae

Nummus monoculatus Morgan 1975 (Fig. 8R, U)
Cyclopsiella sp. Askin 1988a; Fig. 8.9.
Cyclopsiella sp. Dolding 1992; Fig. 6i, m.
Remarks: This species is smaller (less than 100 μm) than *N. similis* (Cookson and Eisenack) Burger.

5. Biostratigraphy and correlation

The stratigraphic distribution of most of the species from the sample assemblages exhibit some major shifts with local biostratigraphical importance (Figs. 3–5), for example, at ca. 20 m from the base, the disappearance of *Odontochitina porifera* and the appearance of *Manumiella coronata* and *M. seelandica* occur. This event is located ca. 25 m below the level where the theropod and decapods occur. The appearance of *Penninsulapollis gillii*, *Proteacidites* spp., *Alterbidinium acutulum*, *Batiacasphaera? reticulata*, *Manumiella seymourensis*, *M. druggii*, *Phelodinium exilicornutum*,

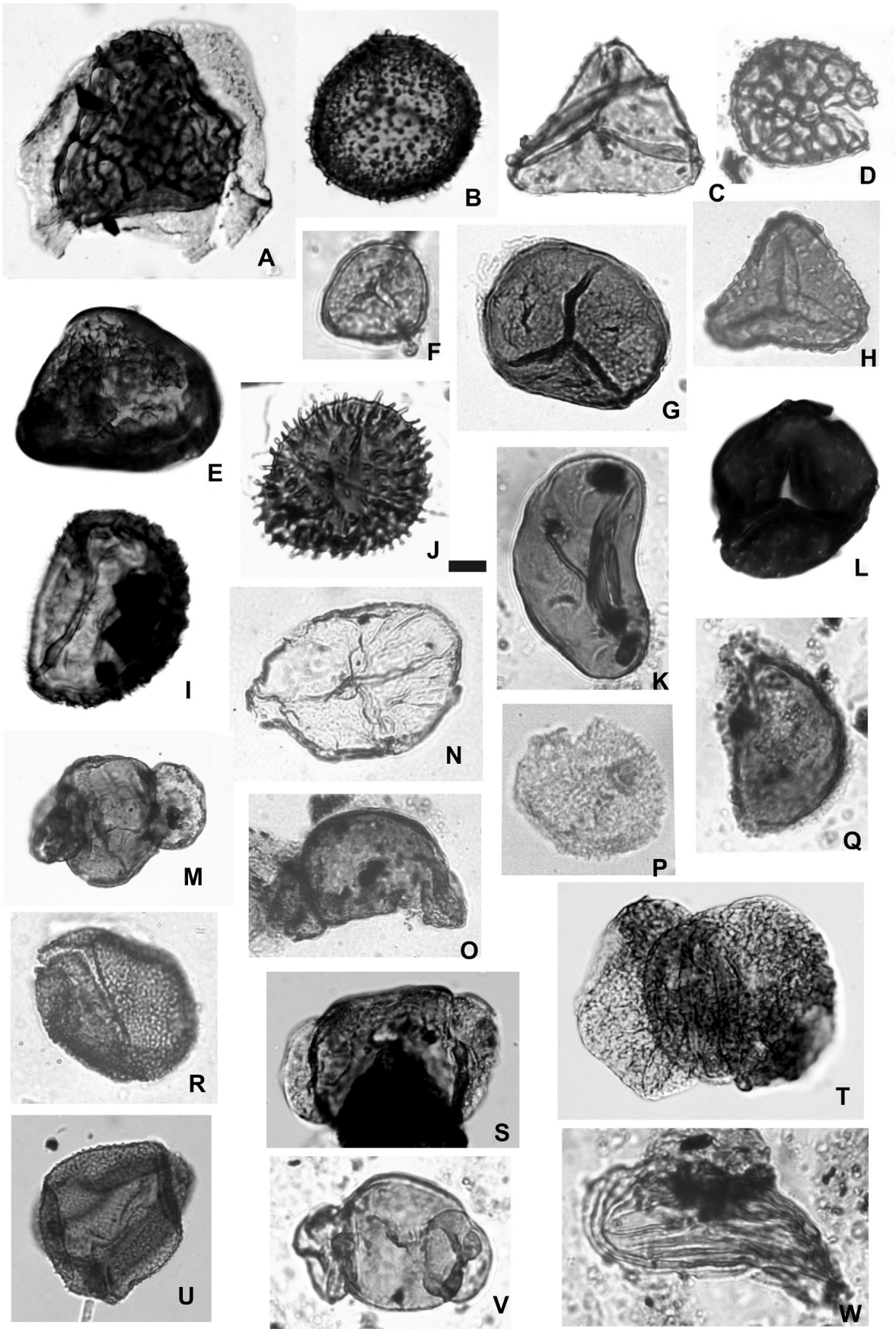
A
B
C
D
E
F
G
H
I
J
K
L
M
N
O
P
Q
R
S
T
U
V
W

Canninginopsis bretonica, *Batiacasphaera rifensis* and a peak of abundance of *Canninginopsis ordospinosa* occur in the basal part of the section as well. Few other species appear from the middle part of the section (e.g., *Battenipollis sectilis*, *Spinidium essoi*, *Pterodinium cretaceum*). Instead, other species show variable frequencies throughout the section (Fig. 5). For example, the most consistently abundant dinoflagellate species are *Trichodinium castaneum–chilensis* complex, *Isabellidinium cretaceum*, *Operculodinium radiculatum*, *Spiniferites ramosus* complex, *Batiacasphaera grandis*, and *Xenascus plotei*, as well as the acritarch *Michrystridium piliferum*, the chlorophycean *Botryococcus brauni*, *Nummus monoculatus* and *Palambages morulosa*, and some podocarpacean (*Podocarpus*, *Phyllocladidites*) and proteacean (*Penninsulapollis gillii*; Figs. 3, 4). Although leiosphaerids and arthropod eggs are abundant throughout the section (Figs. 3, 4), other species show shorter or more restricted vertical distribution (e.g., *Alterbidinium acutulum*, *Canninginopsis ordospinosa*, *C. bretonica*, *Spinidium essoi*, *Senegalinium bicavatum*, *Battenipollis sectilis*), and others appeared intermittently (e.g., *Paleocystodinium granulatum*, *P. golzowense*, *Impagidinium cristatum*, *Manumiella* spp., *Ericipites scabratus*, *Proteacidites*). Many of these changes in abundances are interpreted as variations of environmental conditions (i.e., sea-level changes, nutrients, bloomings) rather than of biostratigraphic significance.

The global stratigraphic range of selected species depicted in Fig. 6 (Chart 1, supplementary online information) reveals that several long-ranging taxa mainly from Campanian–Maastrichtian age occur throughout this section, notably some trilete spores (*Perotrilites majus*), pollen grains (*Podocarpidites*, *Nothofagidites*, *Phyllocladidites*), dinoflagellates (*Isabelidinium cretaceum*, *I. pellucidum*, *Operculodinium radiculatum*, *Spiniferites ramosus* complex) and chlorococcaleans (*Nummus monoculatus* and *Paralecaniella indentata*). Some species appearing in the lowest level show a close relationship with taxa of the Campanian stage (e.g., *Cyclonephelium compactum*, *Diconodinium* sp. cf. *multispinum*, *Xenikoon australis*, *Canningia* sp. 1 in Schiøler and Wilson, *Maduradinium pentagonum*, *Battenipollis sectilis*, *Odontochitina porifera* and *Batiacasphaera grandis*). A few species are known from the Late Maastrichtian or Danian such as *Saeptodinium gravattensis* and *Polypodiisporites favus* (Chart 1, supplementary online information). Key taxa indicate that at least eight dinoflagellate species (*Batiacasphaera rifensis*, *Impagidinium cristatum*, *Isabellidinium cretaceum gravidum*, *Manumiella seymourensis*, *M. seelandica*, *Paleocystodinium pilosum*, *Spinidium essoi*, *Spongodinium reticulatum*) appeared in the early Maastrichtian, whereas *Odontochitina porifera* and *Batiacasphaera grandis* disappeared at the end of this time (Fig. 6). Hence, considering the vertical distribution of selected species, and the biostratigraphic significance of those key species, two informal assemblages are defined and named as lower assemblage *Odontochitina porifera* and upper assemblage *Batiacasphaera grandis* (Figs. 2 and 5). The range of the former is based on the last occurrence (LO) of *Odontochitina porifera*, and the latter is named after a well-represented taxon along the section. Both assemblages suggest an early Maastrichtian age.

However, *Xenascus plotei* and *X. ceratioides* are two dinoflagellate cyst that occur mostly together in the same levels throughout the vertical section (Fig. 4 and Chart 1, supplementary online information), whose age affiliation may be questioned. The former is recorded originally in the mid-Cretaceous (post-Aptian) of the USA, and the latter is widely recorded worldwide (Williams et al., 2004). Mao and Mohr (1992, pl. 6, figs. 10, 12) illustrated *X. ceratioides* in the Campanian of the southern Atlantic Ocean, is better assigned to *X. plotei*. Other specimens of *X. plotei* are illustrated by Smith (1992, fig. 5m) as occurring from the latest Campanian to earliest Maastrichtian of Antarctica. The last occurrence datum (LOD) of *X. ceratioides* is documented up to the early Maastrichtian (Premaor et al., 2010; Chart 1, supplementary online information) and was illustrated by Williams et al. (2004, pl. 27, figs. 4 and 5) by Schiøler and Wilson (1998, pl. 8, fig. 9) from the Coniacian–early Campanian of New Zealand, and by Premaor et al. (2010, fig. 4N) from the Campanian of Brazil. Another Santonian–Campanian record of *X. ceratioides* in England was mentioned but not illustrated by Prince et al. (1999). These taxa are here considered indigenous due to their frequency along the section (Fig. 4, 5 and Chart 1, supplementary online information) and their fine preservation. In contrast, scarce specimens of cosmopolitan dinoflagellate such as *Diconodinium* species (Fig. 4 and Chart 1, supplementary online information), and few miospores (e.g., *Dictyotosporites speciosus*) are Early Cretaceous taxa that are likely reworked from older rocks rather than holdovers in this assemblage. Askin (1990a) and Baldoni (1992) have also documented Early Cretaceous palynomorphs reworked into the Campanian–Maastrichtian of James Ross and Seymour Islands. These assemblages from The Naze (Fig. 2) were correlated to selected biostratigraphic schemes from New Zealand (Roncaglia et al., 1999), Antarctica (Askin, 1988a; Smith, 1992 and others related), Australia (Helby et al., 1987) and microfloras from the southern South Atlantic Ocean (Mao and Mohr, 1992; Mohr and Mao, 1997).

Of these areas, Crame et al. (1991) provided composite stratigraphical sections for the James Ross Basin, integrating paleontological information derived from invertebrates and dinoflagellates, which we utilized for correlation. Our dataset of dinoflagellates and ammonites from The Naze allowed correlation to the lower Cape Lamb Member in the Cape Lamb, Vega and northern James Ross Island regions, based on the co-occurrences of several species, such as the dinoflagellates *Isabellidinium pellucidum*, *I. cretaceum*, *Odontochitina porifera*, *Canninginopsis bretonica*, and the ammonite *Diplomoceras lambi* among others. Species of *Manumiella* were recorded in the upper Cape Lamb Member of the López de Bertodano Formation to its top. The lower Cape Lamb Member was attributed to the uppermost Campanian and lower Maastrichtian (Fig. 2 and its references).

Crame et al. (2004) presented a chronostratigraphy for the 1150 m thick Maastrichtian succession in the James Ross Basin integrating ammonite biostratigraphy and isotopic information. They placed the lower–upper Maastrichtian boundary at a level of 91 m in section DJ.1042 corresponding to the absolute date of 71 ± 0.2 Ma obtained from the middle portion of the Cape Lamb Member (Crame et al., 1999) in the concurrent range portions of the ammonites *Diplomoceras lambi*, *Kitchinites darwini*, and *Gunnarites antarcticus* (Pirrie et al., 1991; Crame et al., 1991; Olivero, 2012).

Fig. 7. Illustration of selected palynomorphs occurring within the lithostratigraphic section containing the theropod dinosaur following the order in Fig. 4. Spores and pollen. Scale bar is 15 μm. A, *Perotrilites majus* (Cookson and Dettmann) Evans, CICYTTP-Pl 292-1: Y32/0. B, *Baculatisporites comaumensis* (Cookson) Potonié, CICYTTP-Pl 919-1: V41/4. C, *Birretisporites potoniaei* Delcourt and Sprumont, CICYTTP-Pl 51-3: X57/2. D, *Retitriletes austroclavatidites* (Cookson) Doring et al. in Krutzsch, CICYTTP-Pl 296-1:A30/0. E, *Cyatheacidites archangelskii* Dettmann, CICYTTP-Pl 293-1: A34/3. F, *Stereisporites regium* (Drozhastichich) Drugg, CICYTTP-Pl 51-1: K34-3. G, *Densoisporites velatus* Weyland and Krieger, CICYTTP-Pl 289-2: W42/4. H, *Ischyosporites volkheimeri* Filatoff, CICYTTP-Pl 296-1: Q37/1. I, *Polypodiisporites* sp., CICYTTP-Pl 289-1:T53/0. J, *Ceratosporites equalis* Cookson and Dettmann, CICYTTP-Pl 286-3: Z38/4. K, *Laevigatosporites major* (Cookson) Krutzsch, CICYTTP-Pl 9-2: F26/4. L, *Cyatheacidites annulatus* Cookson, CICYTTP-Pl 293-1:W57/3 (tetrad). M, *Podocarpidites otagoensis* Couper, CICYTTP-Pl 292-2: R32/0. N, *Triporoletes radiatus* (Dettmann) Playford, CICYTTP-Pl 287-1: E29/4. O, *Podocarpidites rugulatus* Pocknall and Mildenhall, CICYTTP-Pl 296-3: S25/0. P, *Dilwynites granulatus* Harris, CICYTTP-Pl 286-1: V31/0. Q, *Peromonolites bowenii* Couper, CICYTTP-Pl 9-2: K30/1. R, *Longapertites* sp. in Povilauskas et al., CICYTTP-Pl 296-3: X28/3. S, *Podocarpidites rugulatus* Pocknall and Mildenhall, CICYTTP-Pl 293-1: U42/3. T, *Podocarpidites major* Cookson, CICYTTP-Pl 289-1: R44/4. U, *Araucariacites australis* Cookson, CICYTTP-Pl 292-2: V21/3. V, *Phyllocladidites mawsonii* Cookson ex Couper, CICYTTP-Pl 52-3:C38/0. W, *Equisetosporites* sp., 51-2: X51/3.

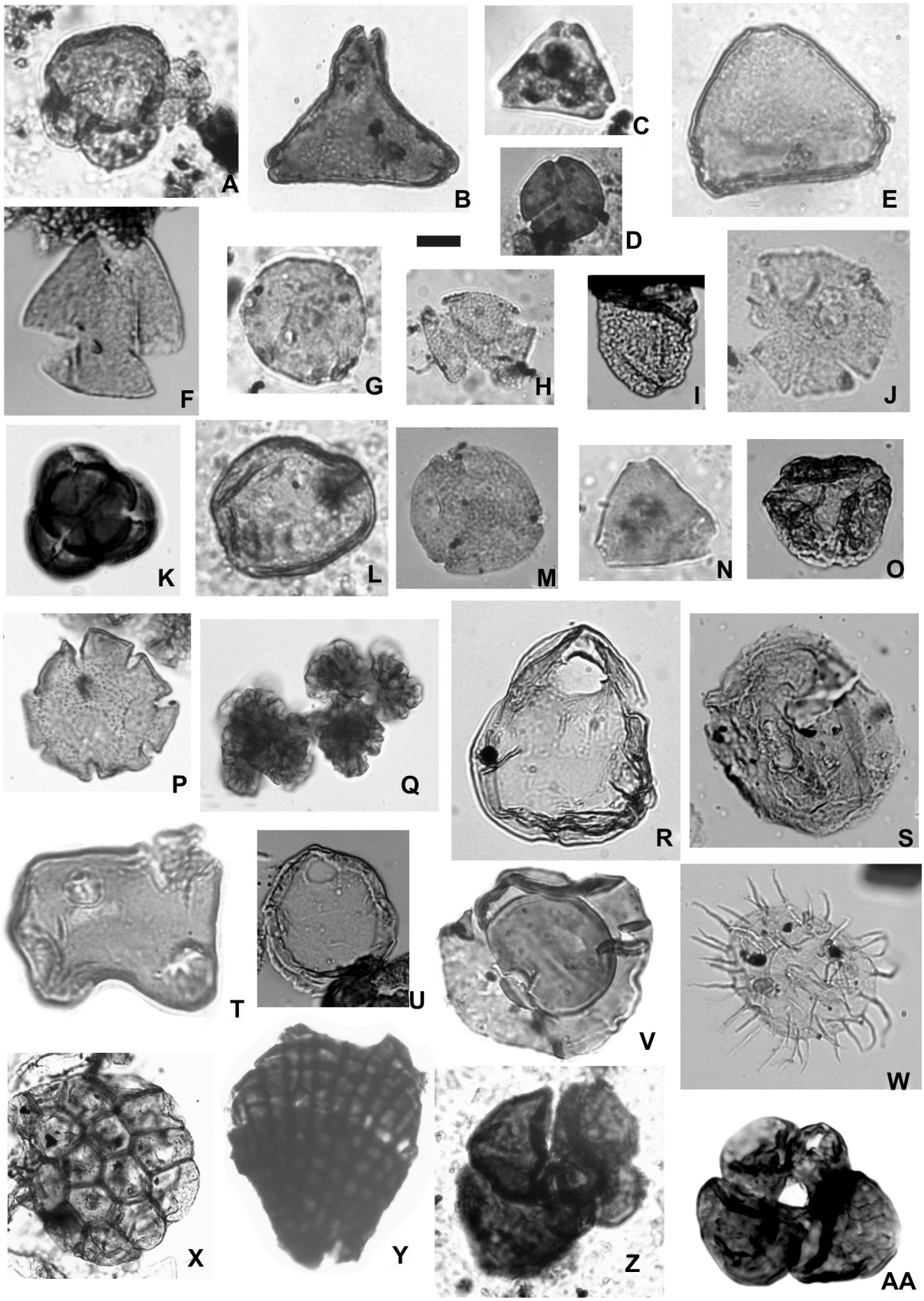

Fig. 8. Illustration of selected palynomorphs occurring within the lithostratigraphic section containing the theropod dinosaur following the order in Fig. 4. Pollen and other remains. Scale bar is 15 μm except for Figs. Q and X that is 20 μm. A, *Microcachrydites antarcticus* Cookson ex Couper, CICYTTP-Pl 10-1: J29/0. B, *Battenipollis sectilis* (Stover) Jarzen and Dettmann, CICYTTP-Pl 292-2: Q32/3. C, *Proteacidites scaboratus* Couper, CICYTTP-Pl 9-3: H27/0. D, *Tricolpites confessus* Stover in Stover and Partridge, CICYTTP-Pl 51-1: L43/0. E,

Although they showed that it extends diachronously across the basin, as it would have been affected by the unconformity at the base of the Sandwich Bluff Member recorded on Cape Lamb.

The co-occurrence of the first two ammonoid taxa allow the attribution of this section to the early Maastrichtian *Gunnarites* biozone after Crame et al. (2004) or Ammonite Assemblage 10 (Fig. 2) in the NG sequence after Olivero (2012). These authors agreed that these sequence stratigraphic framework established for the Santonian–Danian of the James Ross Basin probably represents a low cyclicity frequency of second or third-order cycles. The time involved is probably of the order of 7–8 Ma for the N Sequence, at the beginning of the Santonian to the lower–upper Campanian boundary; about 8–9 Ma for the NG Sequence, upper Campanian–lower Maastrichtian; and about 5 Ma for the MG Sequence, lower Maastrichtian–Danian.

Palynological comparisons with other assemblages of late Campanian–early Maastrichtian age from Vega and James Ross Islands and surrounding areas (Askin, 1988a; Pirrie et al. 1991, 1997; Riding et al., 1992; Smith, 1992; Dolding, 1992; Wood and Askin, 1992) showed a relatively high number of common species mainly ranging from late Campanian to early Maastrichtian, although most of them are extended up to late Maastrichtian (see Figs. 2, 6 and Chart 1, supplementary online information).

The most similar palynofloras are from Vega Island, documented by Smith (1992), who recorded 55 species and, of them, 25 are shared with our assemblages. The early Maastrichtian age of the sample D3122.3 described by Dettmann and Thomson (1987) contained 40 species in common from 63 total species. In Humps Island, the upper Campanian rocks studied by Dolding (1992) yielded 140 species and 40 are here in common, whereas Wood and Askin (1992) from the same place and age, mentioned 43 species and 9 are in common.

The correlation chart presented by Pirrie et al. (1991) for the López de Bertodano Formation in Cape Lamb, Vega Island illustrated a concurrent appearance of *Gunnarites antarcticus* and *Diplomoceras lambi–Kitchinites darwini* with the ranges of dinoflagellates such as *Isabellidinium cretaceum*, *I. pellucidum* and *Canninginopsis bretonica* in their B member. They attributed this assemblage of long-ranging species to the late Campanian and early Maastrichtian. The frequent occurrence of *Manumiella seymourensis* is concurrent with the overlying *Maorites* assemblage in their C member, although this dinoflagellate appears slightly earlier in conjunction with the underlying assemblages as they showed in their chart of occurrences. Other species of *Manumiella* (i.e., *M. seelandica*, *M. bertodano*, *M. coronata*, *M. druggii*) were recorded by Pirrie et al. (1991) later in the late Maastrichtian.

Askin (1988a) studied two samples from a section at The Naze (Fig. 2) that yielded quite similar assemblages to the ones here studied, although few species were mentioned, including *Odontochitina operculata*, *O. spinosa*, *O. porifera*, *Trichodinium castanea*, *Canninginopsis ordospinosa*, and a peridinoid cysts plexus, as well as rare specimens of *Operculodinium radiculatum*, *Paleocystodinium* spp., *Nummus similis*, *Nelsoniella aceras*, *Phelodinium exilicornutum* (Fig. 6), *Triporoletes radiatus*, and *Spiniferites* spp. (see synonymies of species into item 4). On the basis of this assemblage in conjunction with assemblages from Vega and Seymour Islands, Askin (1988a) proposed an informal zonation scheme (Fig. 2). Bowman et al. (2012) restudied the dinoflagellate assemblages from the López de Bertodano Formation on Seymour Island, previously analyzed by Askin (1988a), and proposed a new biozonation of the late Maastrichtian mainly based on the first appearances of *Manumiella* species. The studied section crops out continuously over approximately 70 km^2 with a thickness of ca. 1000 m and is bounded by unconformities with the Haslum Crag Member (uppermost Snow Hill Island Formation) beneath, and with the overlying Sobral Formation (Pirrie et al., 1997; Crame et al., 2004; Olivero et al., 2008). Crame et al. (2004) discussed the Late Maastrichtian age given to the base of the López de Bertodano Formation by Pirrie et al. (1997) based on *Manumiella druggii* and *M. seymouriensis*, and *Grapnelispora evansii*, considered it in error. Both *Manumiella* species were recorded from the late Campanian *Isabellidinium pellucidum* Assemblage up to the late Maastrichtian *Manumiella druggii* Interval Zone (Fig. 2) in New Zealand (Roncaglia et al., 1999). This early appearance is in agreement with the record of both species from the base of the section here studied, and the introduction of other species successively (*M. seelandica*, *M. coronata*, *M.* sp. cf. *M. bertodano*) is in disagreement with the order of appearances of these species presented by Bowman et al. (2012) (Figs. 2, 5 and Chart 1, supplementary online information).

The absence of typically late Maastrichtian marine species, such as *Bosedinia laevigata*, *Cassidium fragile*, *Cerodinium medcalfii*, *Eisenackia reticulata*, and *Palaeoperidinium pyrophorum* (see Askin, 1988a; Bowman et al., 2012, and references therein), indicate an early Maastrichtian age, older in comparison with the palynofloras from the upper Maastrichtian López de Bertodano Formation presented by Bowman et al. (2012). In summary, the age of the section at The Naze, and as a consequence, the age of the theropod, appears more likely early Maastrichtian than late Maastrichtian; moreover, the species occurrences are more likely biostratigraphically controlled rather than paleoecological as indicated by the first occurrence (FOs) of *Batiacasphaera rifensis*, *Impagidinium cristatum*, *Isabellidinium cretaceum gravidum*, *Manumiella seymourensis*, *M. seelandica*, *Paleocystodinium pilosum*, *Spinidium essoi*, and *Spongodinium reticulatum* that are introduced in the early Maastrichtian. In addition, the last occurrence (LOs) of *Odontochitina porifera* and *Batiacasphaera grandis* occur at the end of the early Maastrichtian. Also, the palynofloral evidence is reinforced by the stratigraphic ranges of the two ammonoid species mentioned above (see Figs. 2 and 6).

6. Paleoenvironmental approach based on terrestrial and marine palynomorphs

Marine palynomorphs

Overall, the dominance of marine dinoflagellates in all levels through this section (Figs. 3–5) at The Naze supports the existence of a permanent marine depocentre. The predominance of peridinialean cysts with algal remains (e.g., *Nummus monoculatus*, prasinophytes) and the acritarch *Michrystridium pilosum* within the section, are evidences of more inner neritic settings, close to the paleoshoreline (Chart 2, supplementary online material). *Nummus monoculatus* exhibits an encrusting habit (bentonic), and indicates

Proteacidites tenuiexinus Stover in Stover and Partridge, CICYTTP-Pl 288-1: J26/0. F, *Peninsulapollis gillii* (Cookson) Dettmann and Jarzen, CICYTTP-Pl 291-1: V41/1. G, *Myricipites harrisii* (Couper) Dutta and Sah, CICYTTP-Pl 51-2: O38/4. H, *Peninsulapollis askiniae* Dettmann and Jarzen, CICYTTP-Pl 51-1: M44/1. I, *Liliacidites* sp., CICYTTP-Pl 290-1: Q27/2. J, *Nothofagidites americanus* Zamaloa, CICYTTP-Pl 8-1: X27/2. K, *Ericipites scabratus* Harris, CICYTTP-Pl 295-1: B52/1. L, *Periporopollenites polyoratus* (Couper) Stover in Stover and Partridge, CICYTTP-Pl 51-2: U46/3. M, *Triorites orbiculatus* McIntyre, CICYTTP-Pl 10-2: Z28/2. N, *Proteacidites parvus* Cookson, CICYTTP-Pl 10-1: K30/0. O, *Trichotomosulcites subgranulatus* Couper, CICYTTP-Pl 295-1: S55/0. P, *Nothofagidites saraensis* Menéndez and Caccavari de Filice, CICYTTP-Pl 292-2: Z46/3. Q, *Botryococcus brauni* Kützing, CICYTTP-Pl 289-2: T49/1. R, *Nummus monoculatus* Morgan, CICYTTP-Pl 289-2: V51/1. S, *Paralecaniella indentata* (Deflandre and Cookson) Cookson and Eisenack emend. Elsik, CICYTTP-Pl 293-1: W57/3. T, *Tetraedron* cf. *minimum* (A. Braun) Hansgirg, CICYTTP-Pl 296-1: W32/0. U, *Nummus monoculatus* Morgan, CICYTTP-Pl 291-1: Q20/0. V, *Pterospermella aureolata* (Deflandre and Cookson) Eisenack, CICYTTP-Pl 52-3: C37/0. W, *Michrystridium piliferum* Deflandre, CICYTTP-Pl 292-2: P21/0. X, *Palambages* sp., CICYTTP-Pl 289-2: O58/3. Y, *Asterothyrites* Cookson, CICYTTP-Pl 296-3: L30/0. Z, Foraminiferal lining, CICYTTP-Pl 51-3: V57/0. AA, Foraminiferal lining, CICYTTP-Pl 290-1: D52/1.

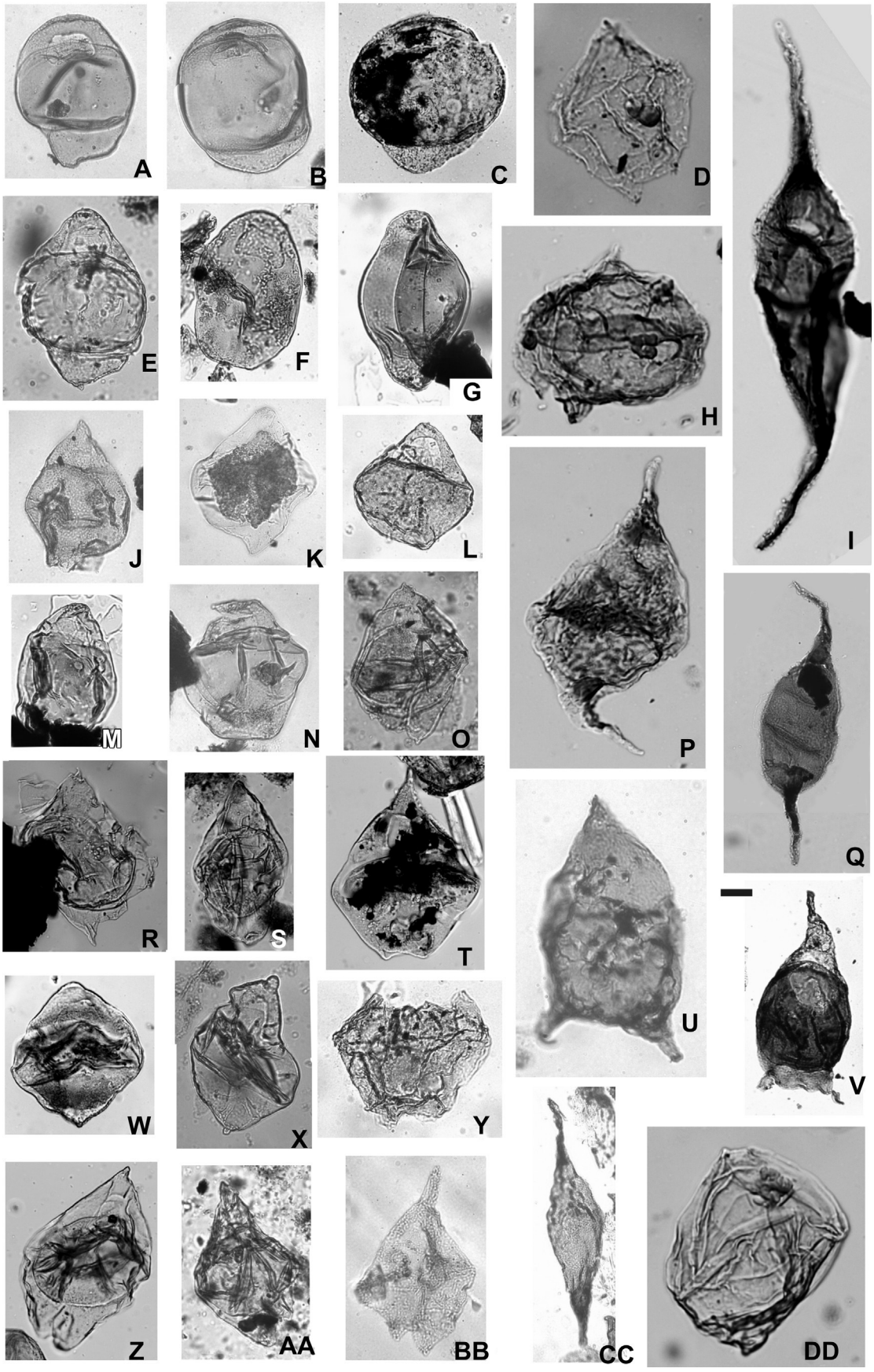

Fig. 9. Illustration of selected palynomorphs occurring within the lithostratigraphic section containing the theropod dinosaur following the order in Fig. 4. Dinoflagellates, Peridiniales. Scale bar is 20 μm for Figs. D, H, I, P, U, DD, and 40 μm for the remaining figures. A, *Isabelidinium cretaceum* (Cookson) Lentin and Williams, CICYTTP-Pl 287-1: L34/4. B,

coastal marine settings; the acritarch is characteristic of the shallowest, inner neritic settings, or partly restricted settings (Duane, 1996; Chart 2, supplementary online material). This occurs at sample AC-14 where a low number of species and dinocysts suggest a restricted environment, where only a limited number of taxa can survive (Figs. 3–5). Conversely, the recovery of dinoflagellates *Spiniferites* and *Impagidinium* (Mudie and Harland, 1996; Prebble et al., 2006) within the section, together with the frequent pyritization of palynomorphs and other marine elements such as organic foraminiferal linings and megafossils (ammonoids and sharks and plesiosaurs), suggest more open water influences (Figs. 3, 4 and Chart 2, supplementary online material). Nevertheless, terrestrial components such as Podocarpaceae, Nothofagaceae, and Chlorophyceae also occur and are abundant in many sample levels, thus indicating the coastal line probably was nearby and a fresh-water influx was permanent, reflecting the surrounding vegetation at any instant in time (Figs. 3, 4 and Charts 1 and 2, supplementary online material). The appearance of the terrestrial dinosaur at AC-26 level (theropod horizon, Fig. 3) suggests the proximity to a coastline; however, its poor preservation may be the result of prolonged transport (although poor preservation is also the result of extensive subaerial degradation).

Variations in abundances of different marine and terrestrial palynomorphs (Fig. 3, MT ratio) reflect the influence of variable terrigenous supplies from deltaic and other terrestrial environments established around the marine depocenter where variable conditions (i.e., local sea-level changes, content of nutrients, bloomings) also would have occurred during the time of deposition. A high percentage of *Trichodinium castanea–chilensis* in three levels of The Naze section (Fig. 3) is interpreted as blooms occurring in a shallow protected environment, probably the result of an increase in nutrients (Edet and Nyong, 1993; Brinkhuis, 1994; Matthiessen, 1995; Mudie and Harland, 1996; Chart 2, supplementary online material). Blooms could be induced by upwelling waters close to the coastline of the continents independently of the seaward currents carrying land-derived materials to the shelf (e.g., Malloy, 1972).

Terrestrial palynomorphs

Cyatheacidites species (tree fern, *Lophosoria* spores) and species of *Nothofagidites*–Podocarpaceae–Proteaceae supports the nearby development of cool-temperate moist rain forest during the Late Cretaceous of Antarctica, similar to the current rain forest to heathland habitats in Central to South America (e.g., Dettmann, 1986; Askin, 1990a; Chart 2 of the supplementary online material). Moreover, the discovery of several tetrads (Fig. 7L) of this species and considering its resistance to long transport owing to its heavy nature (due to its cingulate amb), these cool-temperate forests were likely developed close to the shoreline.

In these forests, other “primitive” endemic communities of angiosperms such as Gunneraceae, Ericaceae, Casuarinaceae, Epacridaceae, Winteraceae and Trimeniaceae occurred adjacent to estuaries or coal forming swamps at high southern paleolatitudes (e.g., Dettmann and Jarzen, 1990; Hill and Scriven, 1995; Wagstaff et al., 2006). Some of these angiosperms are recorded herein in low frequencies (Fig. 3), such as the pollen of Palmae (e.g., *Liliacidites*, *Longapertites*) that suggests warm to temperate conditions in frost-free lowland areas. Palmae pollen was transported by rivers close to the marine environment, as they are not usually transported far from their habitat (e.g., Edet and Nyong, 1993; Chart 2 supplementary online information). The occurrence of isolated and fragmented ascocarps of epiphyllous fungi of Microthyriaceae affinity in three specific levels (Fig. 3) of this section indicates a warm and humid climate in the surrounding terrestrial environments (e.g., Duane, 1996; Kalgutkar and Braman, 2008). Hence, cool to temperate and mainly humid environments were developed during the deposition of The Naze assemblages, which is also supported by several species of miospores, particularly fern spores together with bryophyte and lycophyte spores. The consistently low number of Araucariaceae and other taxa (*Equisetosporites*, Ericaceae) throughout the section would represent more xerophytic environments or minor elements into those forests (Figs. 3, 4 and Chart 2 supplementary online information).

7. Summary and conclusions

Sixteen palynoassemblages were studied from the Cape Lamb Member of the Snow Hill Island Formation at The Naze where a theropod dinosaur was recovered near the middle portion of a 90 m thick section. The assemblages presented moderate diversity and a total of 100 relatively well-preserved species. The main terrestrial groups (32%) are represented by lycophytes (8 species), pteridophytes (15 species), gymnosperms (13 species), angiosperms (21 species) and freshwater chlorococcaleans (3 species). Marine palynomorphs (68%) belong to dinoflagellates (61 species), chlorococcaleans (6 species), and one acritarch (*Michrystridium piliferum*). The vertical distribution of selected species allows the distinction of two informal assemblages, the lower *Odontochitina porifera* assemblage from the base to where it disappears in the lower portion of the section and the upper *Batiacasphaera grandis* assemblage from the highest occurrence of *O. porifera* to the top of the exposed Cretaceous section.

The global stratigraphic ranges of selected palynomorphs suggest an early Maastrichtian age that is also supported by the presence of the ammonoid *Kitchinites darwinii*. These assemblages share many species with latest Campanian–early Maastrichtian palynofloras from Vega and Humps Islands, New Zealand, and elsewhere in the Southern Ocean, establishing good lateral correlation (Fig. 2).

The Cape Lamb, Sanctuary Cliffs and Karlsen Cliffs members of the Snow Hill Island Formation consist of a gradational coarsening and thickening-upward succession of mudstones and sandstones within the James Ross Basin and represent near-shore facies with the overall section shallowing upward (e.g., Crame et al., 1991; Pirrie et al., 1991, 1997). Olivero (2012) interpreted a deltaic wedge that prograded during the time intervals encompassed by Ammonite Assemblages 8–10 for about 80 km to the east, from Santa Marta Cove–Vega Island to Snow Hill–Seymour Islands. During the final regressive phases, the forced regressive strata of

I. cretaceum gravidum Mao and Mohr, CICYTTP-Pl 296-1: E32/4. C, *I. cretaceum oviforme* Mao and Mohr, CICYTTP-Pl 290-1: X51/3. D, *Spinidium essoi* Cookson and Eisenack, CICYTTP-Pl 291-1: Y47/1. E, *Isabelidinium pellucidum* (Deflandre and Cookson) Lentin and Williams, CICYTTP-Pl 10-2: D27/0. F, *Xenikoon australis* Cookson and Eisenack, CICYTTP-Pl 286-3: Z40/3. G, *Amphidiadema nucula* (Cookson and Eisenack) Lentin and Williams, CICYTTP-Pl 286-3: X49/4. H, *Senegalinium bicavatum* Jain and Millepied, CICYTTP-Pl 294-1: O30/4. I, *Paleocystodinium pilosum* Guler et al., CICYTTP-Pl 289-1: O47/0. J, *Chatangiella granulifera* (Manum) Lentin and Williams, CICYTTP-Pl 286-1: Q49/1. K, *Maduradinium pentagonum* Cookson and Eisenack, CICYTTP-Pl 286-1: O49/3. L, *Nelsoniella aceras* Cookson and Eisenack, CICYTTP-Pl 286-3: X43/2. M, *Eurydinium ellipticum* Mao and Mohr, CICYTTP-Pl 286-3: Z56/3. N, *Manumiella druggii* (Stover) Bujak and Davies, CICYTTP-Pl 286-1: P55/0. O, *Manumiella coronata* (Stover) Bujak and Davies, CICYTTP-Pl 9-2: B37/3. P, *Alterbidinium acutulum* (Wilson) Lentin and Williams, CICYTTP-Pl 290-1: M31/3. Q, *Paleocystodinium pilosum* Guler et al., CICYTTP-Pl 289-2: O44/1. R–T, *Manumiella seelandica* (Lange) Bujak and Davies. R, CICYTTP-Pl 293-1: Y41/0. S, CICYTTP-Pl 295-1: H44/1. T, CICYTTP-Pl 289-1: S32/0. U, *Phelodinium exilicornutum* Smith, CICYTTP-Pl 296-1: B37/3. V, *Cerodinium* sp., CICYTTP-Pl 9-2: Z46/3. W–X, *Manumiella seymourensis* Askin. W, CICYTTP-Pl 290-1: X20/1. X, CICYTTP-Pl 10-2: D48/0. Y, *Canninginopsis bretonica* Marshall, CICYTTP-Pl 9-2: S35/4. Z-AA, *Manumiella* sp. cf. *M. bertodano* Thorn et al. Z, CICYTTP-Pl 8-5: M54/2. AA, CICYTTP-Pl 294-1: K54/4. BB, *Canninginopsis ordospinosa* Smith, CICYTTP-Pl 287-1: D34/0. CC, *Palaeocystodinium granulatum* (Wilson) Lentin and Williams, CICYTTP-Pl 296-1: B32/0. DD, *Saeptodinium gravattensis* Harris, CICYTTP-Pl 291-1: T51/0.

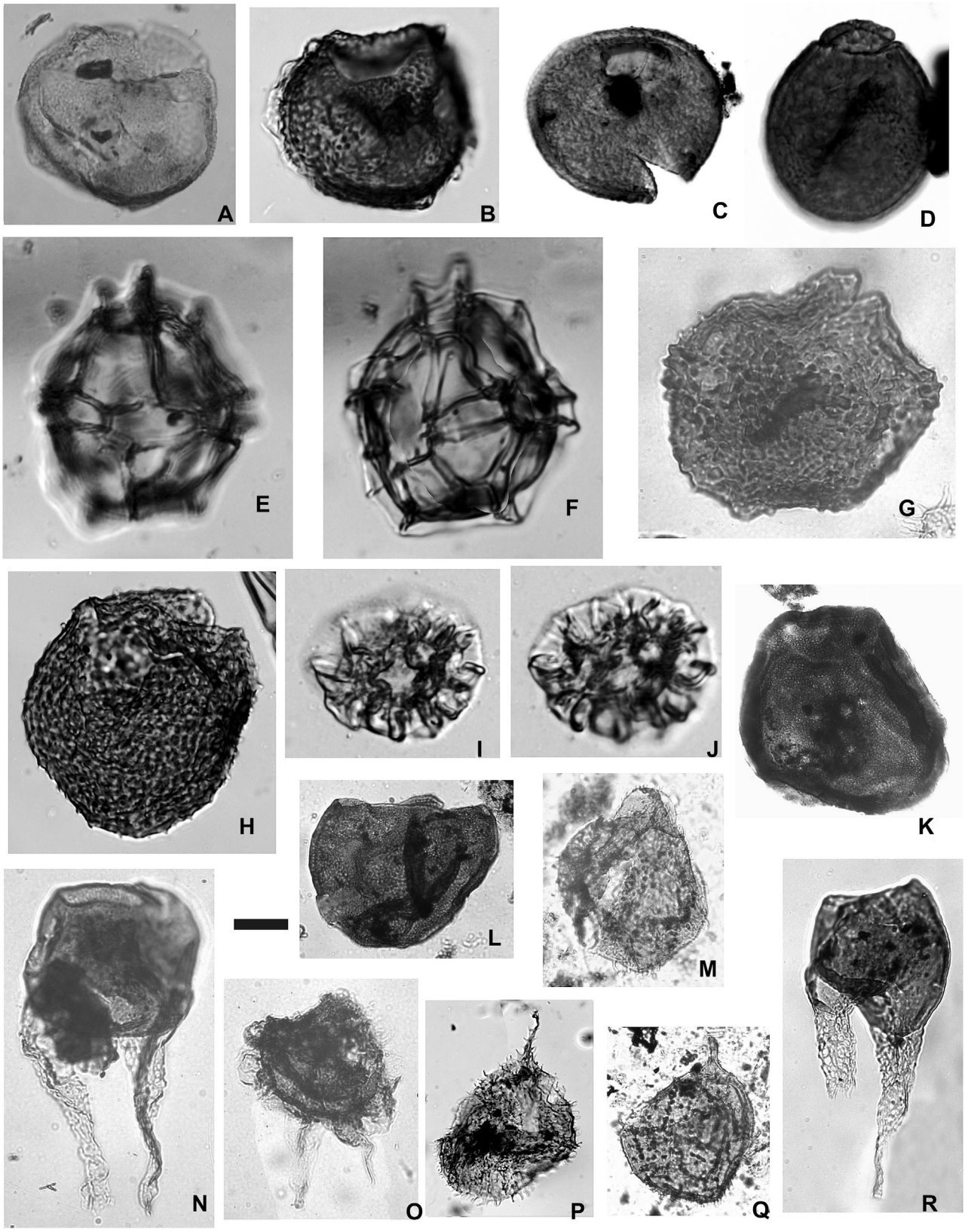

Fig. 10. Illustration of selected palynomorphs occurring within the lithostratigraphic section containing the theropod dinosaur following the order in Fig. 4. Dinoflagellates, Gonyaulacales. Scale bar is 15 μm for Figs. A–D, 10 μm for Figs. E–F, I–J., 20 μm for Figs. G–H, N–O, R, and 40 μm for Figs. K–M, P–Q. A, *Batiacasphaera rifensis* Slimani et al., CICYTTP-Pl 295-1: D56/0. B, *Spongodinium reticulatum* Hultberg, CICYTTP-Pl 290-1: X58/0. C–D, *Batiacasphaera? reticulata* (Davey) Davey. C, CICYTTP-Pl 291-1: X58. D, CICYTTP-Pl 291-1: O33/4. E–F, *Impagidinium cristatum* (May) Lentin and Williams, CICYTTP-Pl 290-1: Z39/4. G, *Canningia* sp.1 Schiøler and Wilson, CICYTTP-Pl 286-1: H58/1. H, *Batiacasphaera rugulata* Schiøler and Wilson, CICYTTP-Pl 294-1: V26/0. I–J, *Pterodinium cretaceum* Slimani et al., CICYTTP-Pl 293-1: J39/2. K–L, *Batiacasphaera grandis* Roncaglia et al. K, CICYTTP-Pl 292-2: X25/0. L, CICYTTP-Pl 9-2: Z22/0. M, P, Q, *Trichodinium castanea* (Deflandre) Clarke and Verdier – *T. chilensis* Troncoso and Doubinger. M, CICYTTP-Pl 8-4: C29/4. P, CICYTTP-Pl 290-1: J20/4. Q, CICYTTP-Pl 51-3: V40/3. N, R, *Odontochitina porifera* Cookson. N, CICYTTP-Pl 286-1: U42/2. R, CICYTTP-Pl 289-2: B24/0. O, *Odontochitina indigena* Marshall, CICYTTP-Pl 287-1: J28/1.

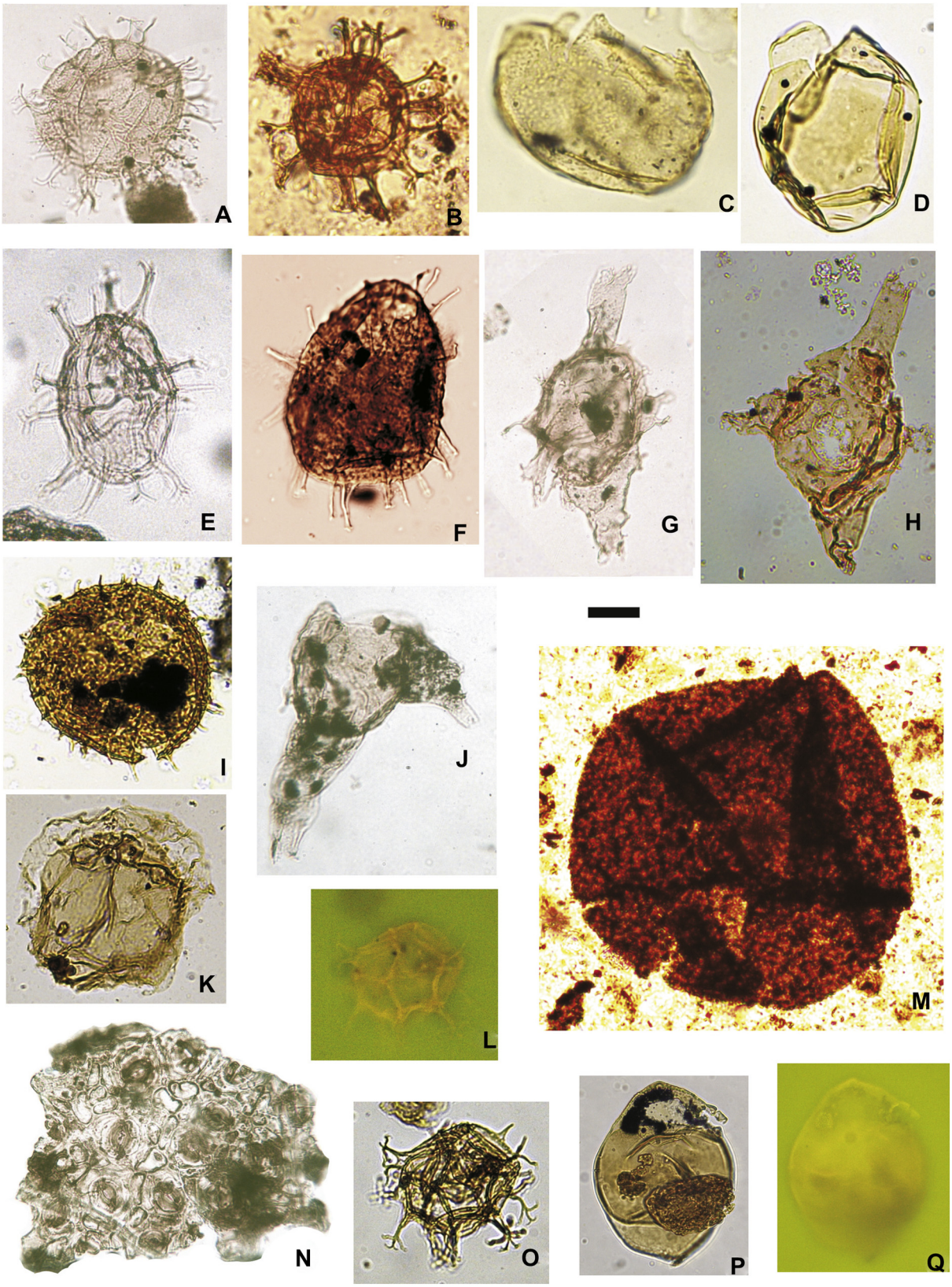

Fig. 11. Illustration of selected palynomorphs occurring within the lithostratigraphic section containing the theropod dinosaur following the order in Fig. 4. Dinoflagellates–Gonyaulacales and others. Scale bar is 20 μm for Figs. A–B, E–H, J, L, O–Q, 15 μm for Figs. C–D, I, K, and 40 μm for Figs. M, N. A–B, L, O, *Spiniferites ramosus* (*ramosus–multibrevis–granosus*) complex (Ehrenberg) Mantell. A, *S. brevis*, CICYTTP-Pl 296-1: Z37/0. B, *S. ramosus*, CICYTTP-Pl 8-4: C42/2. L, *S. ramosus*, CICYTTP-Pl 289-2: T49 (under fluorescence light). O, same specimen in L under transmitted light. C, *Kallosphaeridium parvum* Jan du Chene in Slimani et al., CICYTTP-Pl 292-2: L21/4. D, *Kallosphaeridium? ringnesorium* in Mohr and Mao, CICYTTP-Pl 289-2: K37/4. E, *Spiniferites pseudofurcatus* (Klump) Sarjeant, CICYTTP-Pl 287-1: Z46/3. F, *Operculodinium radiculatum* Smith, CICYTTP-Pl 293-1: W32/3. G, *Xenascus ceratioides* (Deflandre) Davey and Verdier. G, CICYTTP-Pl 296-1: W39/3. H, J, *Xenascus plotei* Below. H, CICYTTP-Pl 10-2: V45/3. J, CICYTTP-Pl 296-1: W28/0. I, *Operculodinium centrocarpum* (Deflandre and Cookson) Wall, CICYTTP-Pl 289-3: Z30/3. M, Arthropod egg, CICYTTP-Pl 51-3: T51. L, *Membranilarnacia densa* Cookson and Eisenack, CICYTTP-Pl 288-2: S55/4. N, Cuticle of Bennettitalean affinity, CICYTTP-Pl 296-1: K25/2. P–Q, *Isabelidinium pellucidum* (Deflandre and Cookson) Lentin and Williams. P, CICYTTP-Pl 289-2: U28/0 (under fluorescence light). Q, same specimen in P under transmitted light.

the Haslum Crag Sandstone suggest that the shoreline was at that time located near Seymour Island (Fig. 2; see also Olivero et al., 2008). Smith (1992) interpreted that the Cape Lamb Member at Vega Island (lowest Maastrichtian) was deposited in a low-energy shelf setting, below storm wave base. The inferred sea-level curve presented by Olivero (2012) for this NG sequence shows for the late Campanian Ammonite Assemblages (AA) 8 a progressive transgressive trend and a regressive trend from the AA 9 to AA 10.

Following the sequence stratigraphic framework of Olivero (2012), our palynoassemblage along the 90 m section of the Cape Lamb Member (Fig. 3) equates to the 8–9 Ma NG Sequence (see also Crame et al., 2004) and should correspond to its Ammonite Assemblage 10 of earliest Maastrichtian age based on the concurrent ranges of ammonoids and palynomorphs documented in the studied section (see Figs. 2, 3 and 6). The Naze section was probably deposited during 1–2 Ma (4th or 5th order in Miall, 1996), in a low-energy shelf setting, based on the lithological composition, thickness of the section, and the palynological information discussed above. The dominance or frequent presence of dinoflagellates throughout the section supports the general interpretation of a shelf marine depocenter. The quali-quantitative variations of dinoflagellates (Figs. 3–5) reflect environmental changes, mainly shoreline shifts that influenced the proximal–distal trend of the permanent marine depocenter at The Naze. The inferred sea level curve based on palynological and other paleontological evidence along the section, points to an important role of local sea level changes in controlling the abundance and composition of vegetation probably largely due to the amount of coastal plain available for colonization. These small-scale temporal changes could be related to Milankovitch cycles in a regional and larger scale cooling and regressive event that would have occurred from the end of the Campanian through the early Maastrichtian.

Based on The Naze section (see Fig. 3), the terrestrial environments surrounding this depocenter were represented by podocarp–*Nothofagus* rainforests established mainly in lowlands with other angiosperm groups and ferns developed in understories, under highly humid and temperate to cool-temperate conditions. Lycophytes and bryophytes and subordinated elements (e.g., Proteaceae, *Battenipollis*, Liliaceae, Palmae, Microthyriaceae, and other herb–shrub dicotyledonous species), likely endemic (see Askin, 1989), were mostly related to the vegetation along riparian floodplains, swamps (with *Stereisporites* and Lycopodiales) and lakes (with Chlorophytes and fresh water dinoflagellates *Saeptodinium*) that were fringing estuaries with brackish waters (*Michrystridium*, some Chlorophytes and few peridinalean species) to the shallow marine shelf (the permanent depocenter). These communities were developed under cool-temperate, frost-free and high-rainfall conditions (Dettmann, 1986, 1989; Askin, 1990a, 1990b; Jarzen and Dettmann, 1992; Crame, 1992; Hill and Scriven, 1995). Well-defined growth rings within fossil wood samples (*Araucarioxylon* Krausel) recovered from Lachman Crags and The Naze (James Ross Island) showed that this climate was markedly seasonal (Francis, 1986, 1991).

Bowman et al. (2012) presented a paleobiogeographical synthesis including a proposal of a South Polar Province characteristic of cool waters embracing northwestern Antarctica (James Ross Basin), the East Tasman Plateau, New Zealand and southern South America and Australia for the late Maastrichtian to earliest Paleocene. The marine endemic palynomorphs in our assemblages (e.g., *Manumiella seymourensis*, *Operculodinium exilicornutum*, *Batiacasphaera grandis*) confirm the inclusion of this area in this phytocore during the early Maastrichtian. Some marine cosmopolitan dinoflagellate species here recorded (e.g., *Chatangiella granulifera*, *Isabellidinium pellucidum*, *Isabellidinium cooksoniae*, *Xenascus plotei*, *Xenascus ceratioides*, *Spiniferites ramosus*, *Operculodinium centrocarpum*) indicate a relatively free connection of the western regions along the Paleopacific Ocean to other regions of the World. This is also reinforced by the record of *Odontochitina porifera* in the Campanian of southernmost Brazil (Premaor et al., 2010), and by *Chatangiella granulifera* recorded in the basal part of the The Naze section (Fig. 4), which has been suggested to be characteristic of cold waters of the North Polar region (Canadian Arctic and Siberia) during the latest Cretaceous (Harker et al., 1990).

Acknowledgments

The authors would like to sincerely thank the Instituto Antárctico Argentino and the National Science Foundation, Office of Polar Programs, who were responsible for the support of the expeditions (NSF grants awarded to J.E. Martin (OPP#0087972) and J.A. Case (OPP#0003844)). This research would not have been possible without the collaboration from Dr. Judd A. Case, Eastern Washington University. Dr. J. Foster Sawyer (SD School of Mines and Technology), collaborated in measuring and sampling the section in Antarctica. M. Di Pasquo acknowledges the Fulbright Scholarship Program and CONICET of Argentina for providing her the opportunity for cooperation with colleagues from USA and for continuing collaboration. Support from home institutions is greatly appreciated (e.g. ANPCyT Pict 07-36166). Captain Mike Terminal and crew of the Lawrence M. Gould research vessel are thanked for their congeniality and for transportation to James Ross Island. Mr. John Evans and his staff in Raytheon Polar made every effort to make our sojourn possible, safe, and comfortable. We thank all our field companions, Dr. Marcelo Reguero, Dr. J. Foster Sawyer, Dr. Allen J. Kihm, Dr. Jennifer Hargrave, Dr. Robert Meredith, Ms. Amanda Person, Dr. Wayne Thompson, Ms. Melissa Rider, Dr. Kristin van Konynenburg, Mr. Joe Pettit, Mr. Dan Martin, and Ms. Lucy Bledsoe, whose dedication to science and congeniality during extremely difficult field conditions are the cornerstone of this research. Dr. Wayne Thompson aided further in the sketch of the outcrop for which we are thankful. The authors thank to the anonimous reviewers and the Editor E.A.M. Koutsoukos for their suggestions that allowed us to improve our manuscript.

References

Askin, R.A., 1988a. Campanian to Paleocene palynological succession of Seymour and adjacent islands, northeastern Antarctic Peninsula. In: Feldmann, R.M., Woodburne, M.O. (Eds.), Geology and paleontology of Seymour Island, Antarctic Peninsula, Memoir Geological Society of America, 169, pp. 131–153.

Askin, R.A., 1988b. The palynological record across the Cretaceous/Tertiary transition on Seymour Island, Antarctica. Geological Society of America Memoir 169, 155–162.

Askin, R.A., 1989. Endemism and heterochroneity in the Late Cretaceous (Campanian) to Paleocene palynofloras of Seymour Island, Antarctica: implications for origins, dispersal and palaeoclimates of southern floras. In: Crame, J.A. (Ed.), Origins and Evolution of the Antarctic Biota, Geological Society of London Special Publication, 47, pp. 107–119.

Askin, R.A., 1990a. Campanian to Paleocene spore and pollen assemblages of Seymour Island, Antarctica. Review of Palaeobotany and Palynology 65, 105–113.

Askin, R.A., 1990b. Cryptogam spores from the upper Campanian and Maastrichtian of Seymour Island, Antarctica. Micropaleontology 36, 141–156.

Askin, R.A., 1994. Monosulcate angiosperm pollen from the López de Bertodano Formation (upper Campanian–Maastrichtian–Danian) of Seymour Island, Antarctica. Review of Palaeobotany and Palynology 81, 151–164.

Askin, R.A., 1999. *Manumiella seymourensis* new species, a stratigraphically significant dinoflagellate cyst from the Maastrichtian of Seymour Island, Antarctica. Journal of Paleontology 73, 373–379.

Baldoni, A., 1992. Palinologia de la Formación Santa Marta, Cretácico Superior de la Isla James Ross, Antártida. In: Rinaldi, C.A. (Ed.), Geología de la Isla James Ross. Instituto Antártico Argentino, Buenos Aires, pp. 359–374.

Baldoni, A.M., Barreda, V., 1986. Estudio palinológico de las Formaciones López de Bertodano y Sobral, isla Vicecomodoro Marambio, Antártida. Boletín de la IG-USP, Instituto de Geociencias, Universidad de San Paulo 17, 89–98.

Baldoni, A.M., Medina, F., 1989. Fauna y microflora del Cretácico en Bahía Brandy, isla James Ross, Antártida. Serie Científica INACH 39, 43–58.

Barreda, V.D., Palamarczuk, S., Medina, F., 1999. Palinología de la Formación Hidden Lake (Coniaciano-Santoniano), isla James Ross, Antártida. Revista Española de Micropaleontología 31, 53–72.
Below, R., 1981. Dinoflagellaten-Zysten aus dem oberen Hauterive bis unteren Cenoman Süd-West-Marokkos. Paläeontographica, Abteilung B 176, 1–145.
Bowman, V.C., Francis, J.E., Riding, J.B., Hunter, S.J., Haywood, A.M., 2012. A latest Cretaceous to earliest Paleogene dinoflagellate cyst zonation from Antarctica, and implications for phytoprovincialism in the high southern latitudes. Review of Palaeobotany and Palynology 171, 40–56.
Brinkhuis, H., 1994. Late Eocene to early Oligocene dinoflagellate cysts from the Priabonian type-area (northeast Italy): biostratigraphy and palaeoenvironmental interpretation. Palaeogeography, Palaeoclimatology, Palaeoecology 107, 121–163.
Case, J.A., Martin, J.E., Chaney, D.S., Reguero, M., 2003. Late Cretaceous Dinosaurs from the Antarctic Peninsula: Remnant or Immigrant Fauna. Journal Vertebrate Paleontology 23 (3 suppl.), 39A.
Case, J.A., Martin, J.E., Reguero, M., 2007. A Dromaeosaur from the Maastrichtian of James Ross Island and the Late Cretaceous Antarctic Dinosaur Fauna. In: Cooper, A.K., Raymond, C.R., et al. (Eds.), Antarctica: A Keystone in a Changing World. Online Proceeding 10th International Symposium on Antarctic Earth Sciences. US Geological Survey, Open-File Report, 2007-1047, 4 p.
Clarke, R.F.A., Verdier, J.-P., 1967. An investigation of microplankton assemblages from the Chalk of the Isle of Wight, England. Verhandelingen der Koninklijke Nederlandse Akademie van Wetenschappen, Afdeeling Natuurkunde, Eerste Reeks 24, 1–96.
Couper, R.A., 1953. Upper Mesozoic and Cainozoic spores and pollen grains from New Zealand. New Zealand Geological Survey, Palaeontological Bulletin 22, 1–77.
Crame, J.A., 1992. Late Cretaceous palaeoenvironments and biotas: an Antarctic Perspective. Antarctic Science 4, 371–382.
Crame, J.A., Francis, J.E., Cantrill, D.J., Pirrie, D., 2004. Maastrichtian stratigraphy of Antarctica. Cretaceous Research 25, 411–423.
Crame, J.A., McArthur, J.M., Pirrie, D., Riding, J.B., 1999. Strontium isotope correlation of the basal Maastrichtian Stage in Antarctica to the European and US biostratigraphic schemes. Journal of the Geological Society of London 156, 957–964.
Crame, J.A., Pirrie, D., Riding, J.B., Thomson, M.R.A., 1991. Campanian-Maastrichtian (Cretaceous) stratigraphy of the James Ross Island area, Antarctica. Journal of the Geological Society of London 148, 1125–1140.
Davey, R.J., 1969. Some dinoflagellate cysts from the Upper Cretaceous of northern Natal, South Africa. Palaeontologia Africana 12, 1–23.
Davey, R.J., 1979. Two new Early Cretaceous dinocyst species from the northern North Sea. Palaeontology 22, 427–437.
Delcourt, A., Sprumont, G., 1955. Les spores et grains de pollen du Wealdien du Hainaut. Memoires de la Societe Geologique de Belgique, nouvelle series 5, 1–73.
Dettmann, M.E., 1986. Significance of the Cretaceous–Tertiary spore genus *Cyatheacidites* in tracing the origin and migration of *Lophosoria* (Filicopsida). Special Paper on Palaeontology 35, 63–94.
Dettmann, M.E., 1989. Antarctica: Cretaceous cradle of austral temperate rainforests? In: Crame, J.A. (Ed.), Origins and Evolution of the Antarctic Biota, Geological Society Special Publication, 47, pp. 89–105.
Dettmann, M.E., Jarzen, D.M., 1990. The Antarctic/Australasian rift valley: Late Cretaceous cradle of northeastern Australasian relicts? Review of Palaeobotany and Palynology 65, 131–144.
Dettmann, M.E., Playford, G., 1968. Taxonomy of some Cretaceous spores and pollen grains from eastern Australia. Proceedings of the Royal Society of Victoria 81, 69–94.
Dettmann, M.E., Thomson, M.R.A., 1987. Cretaceous palynomorphs from the James Ross Island area, Antarctica — a pilot study. British Antarctic Survey Bulletin 77, 13–59.
Dolding, P.J.D., 1992. Palynology of the Marambio Group (Upper Cretaceous) of northern Humps Island. Antarctic Science 4, 311–326.
Duane, A.M., 1996. Palynology of the Byers Group (Late Jurassic–Early Cretaceous) of Livingston and Snow islands, Antarctic Peninsula: its biostratigraphical and palaeoenvironmental significance. Review of Palaeobotany and Palynology 91, 241–281.
Edet, J.J., Nyong, E.E., 1993. Depositional environments, sea-level history and paleobiogeography of the late Campanian–Maastrichtian on the Calabar flank, SE Nigeria. Palaeogeography, Palaeoclimatology, Palaeoecology 102, 161–175.
Fensome, R.A., MacRae, R.A., Williams, G.L., 2008. DINOFLAJ2, Version 1. In: American Association of Stratigraphic Palynologists, Data Series no. 1. Document generated 2008-07-30.
Francis, J.E., 1986. Growth rings in Cretaceous and Tertiary wood from Antarctica and their palaeoclimatic implications. Palaeontology 29, 665–684.
Francis, J.E., 1991. Palaeoclimatic significance of Cretaceous–early Tertiary fossil forests of the Antarctic Peninsula. In: Thomson, M.R.A., Crame, A.J., Thomson, J.W. (Eds.), Geological evolution of Antarctica. Cambridge University Press, Cambridge, pp. 623–627.
Harker, S.D., Sarjeant, W.A.S., Caldwell, W.G.E., 1990. Late Cretaceous (Campanian) Organic-Walled Microplankton from the interior plains of Canada, Wyoming and Texas: biostratigraphy, palaeontology and palaeoenvironmental interpretation. Palaeontographica Abeitlung 219, 1–243.
Helby, R., Morgan, R., Partridge, A.D., 1987. A palynological zonation of the Australian Mesozoic. Memoir of the Association of Australasian Palaeontologists 4, 1–94.
Hill, R.S., Scriven, L.J., 1995. The angiosperm-dominated woody vegetation of Antarctica: a review. Review of Palaeobotany and Palynology 68, 175–198.
Hultberg, S.U., 1985. Danian dinoflagellate zonation, the C-T boundary, and the stratigraphical position of the Fish Clay in southern Scandinavia. In: Hultberg, S.U. (Ed.), Dinoflagellate Studies of the Upper Maastrichtian and Danian in Southern Scandinavia. Department of Geology, University of Stockholm, Stockholm, Sweden, pp. 56–82 [Published thesis].
Ioannides, N.S., McIntyre, D.L., 1980. A preliminary palynological study of the Caribou Hills outcrop section along the Mackenzie River, District of Mackenzie. Current Research, Part A. Geological Survey of Canada, Paper 80–1A, pp. 197–208.
Jarzen, D.M., Dettmann, M.E., 1992. Structure and form of Austral Cretaceous Normapolles-like pollen. Geobios 25, 569–583.
Kalgutkar, R.M., Braman, D.R., 2008. Santonian to ?earliest Campanian (Late Cretaceous) fungi from the Milk River Formation, Southern Alberta, Canada. Palynology 32, 39–61.
Lentin, J.K., Williams, G.L., 1981. Fossil dinoflagellates: index to genera and species (1981 edition). In: Bedford Institute of Oceanography, Report Series, no. BI-R-81–12, 345 p.
Malloy, R.E., 1972. An upper cretaceous dinoflagellate cyst lineage from Gabon, West Africa. Geoscience and Man 4, 57–65.
Mao, S., Mohr, B.A.R., 1992. Late Cretaceous dinoflagellate cysts (?Santonian–Maestrichtian) from the southern Indian Ocean (Hole 748C). In: Wise, S.W., Schlich, R., et al. (Eds.), Proceedings of the Ocean Drilling Program: Scientific Results. College Station, Texas, 120, pp. 307–341.
Marenssi, S., Guler, V., Casadío, S., Guerstein, R., Papú, O., 2004. Sedimentology and palynology of the Calafate Formation (Maastrichtian), Austral Basin, Southern Patagonia, Argentina. Cretaceous Research 25, 907–918.
Marshall, N.G., 1988. A Santonian dinoflagellate assemblage from the Gippsland Basin, southeastern Australia. In: Jell, P.A., Playford, G. (Eds.), Palynological and Palaeobotanical Studies in Honour of Basil E. Balme, Memoir of the Association of Australasian Palaeontologists, 5, pp. 195–215.
Martin, J.E., Crame, J.A., 2006. Paleobiological Significance of High-Latitude Late Cretaceous Vertebrate Fossils from the James Ross Basin, Antarctica. In: Francis, J.E., Pirrie, D., Crame, J.A. (Eds.), Cretaceous-Tertiary High-Latitude Paleoenvironments, James Ross Basin, Antarctica, Geological Society of London, Special Publication, 258, pp. 109–124.
Martin, J.E., Bell G.L., Jr., Case, J.A., Chaney, D.S., Fernandez, M.A., Gasparini, Z., Reguero, M., Woodburne, M.O., 2002. Mosasaurs (Reptilia) from the Late Cretaceous of the Antarctic Peninsula. In: Gamble, J.A., Skinner, D.N.B., Henrys, S. (Eds.), Antarctica at the Close of a Millennium. 8th International Symposium on Antarctic Earth Sciences, Bulletin of the Royal Society New Zealand, 35, pp. 293–299.
Martin, J.E., Sawyer, J.F., Reguero, M., Case, J.A., 2007. Occurrence of a Young Elasmosaurid Plesiosaur Skeleton from the Late Cretaceous (Maastrichtian) of Antarctica. In: Cooper, A.K., Raymond, C.R., et al. (Eds.), Antarctica: A Keystone in a Changing World. Online Proceeding 10th International Symposium on Antarctic Earth Sciences. US Geological Survey, Open-File Report., 2007-1047, 4 p.
Matthiessen, J., 1995. Distribution patterns of dinoflagellate cyst and other organic-walled microfossils in recent Norwegian-Greenland Sea sediments. Marine Micropaleontology 24, 307–334.
Miall, A., 1996. The geology of fluvial deposits: sedimentary facies, basin analysis and petroleum geology. Springer-Verlag, Berlin, 582 p.
Mohr, B.A.R., Mao, S., 1997. Maastrichtian dinocyst floras from Maud Rise and Georgia Basin (Southern Ocean): their stratigraphic and paleoenvironmental implications. Palynology 21, 41–65.
Morgan, R., 1975. Some Early Cretaceous organic-walled microplankton from the Great Australian Basin, Australia. Journal and Proceedings of the Royal Society of New South Wales 108, 157–167.
Mudie, P.J., Harland, R., 1996. Aquatic Quaternary. In: Jansonius, J., McGregor, D.C. (Eds.), Palynology: Principles and Applications. American Association of Stratigraphic Palynologists Foundation, Dallas, pp. 843–877.
Olivero, E.B., 2012. Sedimentary cycles, ammonite diversity and palaeoenvironmental changes in the Upper Cretaceous Marambio Group, Antarctica. Cretaceous Research 34, 348–366.
Olivero, E.B., Medina, F.A., 2000. Patterns of Late Cretaceous ammonite biogeography in southern high latitudes: the Family Kossmaticeratidae in Antarctica. Cretaceous Research 21, 269–279.
Olivero, E.B., Ponce, J.J., Martinioni, D.R., 2008. Sedimentology and architecture of sharp-based tidal sandstones in the Upper Marambio Group, Maastrichtian of Antarctica. Sedimentary Geology 210, 11–26.
Pirrie, D., Crame, J.A., Riding, J.B., 1991. Late Cretaceous stratigraphy and sedimentology of Cape Lamb, Vega Island, Antarctica. Cretaceous Research 12, 227–258.
Pirrie, D., Crame, J.A., Lomas, S.A., Riding, J.B., 1997. Late Cretaceous stratigraphy of the Admiralty Sound region, James Ross Basin, Antarctica. Cretaceous Research 18, 109–137.
Pirrie, D., Duane, A.M., Riding, J.B., 1992. Jurassic–Tertiary stratigraphy and palynology of the James Ross Basin: a review and introduction. Antarctic Science 4 (3), 259–266.
Playford, G., 1971. Palynology of Lower Cretaceous (Swan River) strata of Saskatchewan and Manitoba. Palaeontology 14, 533–565.
Prebble, J.G., Hannah, M.J., Barrett, P.J., 2006. Changing Oligocene climate recorded by palynomorphs from two glacio-eustatic sedimentary cycles, Cape Roberts Project, Victoria Land Basin, Antarctica. Palaeogeography, Palaeoclimatology, Palaeoecology 231, 58–70.
Premaor, E., Souza, P.A., Arai, M., Helenes, J., 2010. Palinomorfos do Campaniano (Cretáceo Superior) da Bacia de Pelotas, Rio Grande do Sul: implicações bioestratigráficas e paleoambientais. Pesquisas em Geociências 37, 63–79.

Raine, J.I., Mildenhall, D.C., Kennedy, E.M., 2011. New Zealand fossil spores and pollen: an illustrated catalogue, 4th edition. In: GNS Science miscellaneous series no. 4 http://data.gns.cri.nz/sporepollen/index.htm.
Riding, J.B., Keating, J.M., Snape, M.G., Newham, S., Pirrie, D., 1992. Preliminary Jurassic and Cretaceous dinoflagellate cyst stratigraphy of the James Ross Island area, Antarctic Peninsula. Newsletter on Stratigraphy 26, 19–39.
Romero, E.G., 1977. Polen de Gimnospermas y Fagaceas de la Formación Río Turbio (Eoceno), Santa Cruz, Argentina. Fundación Educacional de Ciencia y Cultura Edit., 223 p.
Roncaglia, L., Field, B.D., Raine, J.I., Schiøler, P., Wilson, G.S., 1999. Dinoflagellate biostratigraphy of Piripauan–Haumurian (Upper Cretaceous) sections from northeast South Island, New Zealand. Cretaceous Research 20, 271–314.
Schiøler, P., Wilson, G.J., 1998. Dinoflagellate biostratigraphy of the middle Coniacian–lower Campanian (Upper Cretaceous) in south Marlborough, New Zealand. Micropaleontology 44, 313–349.
Slimani, H., Louwye, S., Toufiq, A., Verniers, J., De Coninck, J., 2008. New dinoflagellate cyst species from Cretaceous/Palaeogene boundary deposits at Ouled Haddou, south-eastern Rif, Morocco. Cretaceous Research 29, 329–344.
Sluijs, A., Brinkhuis, H., Williams, G.L., Fensome, R.A., 2009. Taxonomic revision of some Cretaceous–Cenozoic spiny organic-walled peridiniacean dinoflagellate cysts. Review of Palaeobotany and Palynology 154, 34–53.
Smith, S.W., 1992. Microplankton from the Cape Lamb Member, López de Bertodano Formation (Upper Cretaceous), Cape Lamb, Vega Island. Antarctic Science 4, 337–353.
Thorn, V.C., Riding, J.B., Francis, J.E., 2009. The Late Cretaceous dinoflagellate cyst *Manumiella* — biostratigraphy, systematics and palaeoecological signals in Antarctica. Review of Palaeobotany and Palynology 156, 436–448.
Troncoso, A., Doubinger, J., 1980. Dinoquistes (Dinophyceae) del limite Cretacico-Tertiario del pozo de Ganso No. 1 (Magallanes, Chile). In: Actas II Congreso Argentino de Paleontología y Biostratigrafía y I Congreso Latinamericano de Paleontología, Buenos Aires, 1978, 2, pp. 93–125.
Wagstaff, B.E., Gallagher, S.J., Lanigan, K.P., 2006. Late Cretaceous palynological correlation and environmental analyses of fluvial reservoir facies of the Tuna Field, Gippsland Basin, southeast Australia. Review of Palaeobotany and Palynology 138, 165–186.
Williams, G.L., Brinkhuis, H., Pearce, M.A., Fensome, R.A., Weegink, J.W., 2004. Southern ocean and global dinoflagellate cyst events compared: index events for the Late Cretaceous–Neogene. In: Exon, N.F., Kennett, J.P., Malone, M.J. (Eds.), Proceedings of the Ocean Drilling Program Scientific Results, 189, pp. 1–98.
Wood, S.A., Askin, R.A., 1992. Dinoflagellate cysts from the Marambio Group (Upper Cretaceous) of Humps Island. Antarctic Science 4, 327–336.
Wrenn, J.H., Hart, G.F., 1988. Paleogene dinoflagellate cyst biostratigraphy of Seymour Island, Antarctica. Geological Society of America Memoir 169, 321–447.

Appendix A. Supplementary data

Supplementary data related to this article can be found at http://dx.doi.org/10.1016/j.cretres.2013.07.008.

Appendix B

List of taxa documented in the Snow Hill Island Formation at The Naze, arranged by major groups in alphabetical order. The reference of illustrated specimens in Figs. 7–11 (mostly following the order in Fig. 4) is included. See full authority in Fig. 4.

Spores

Baculatisporites comaumensis (Cookson) Potonié (Fig. 7B)
Biretisporites potoniaei Delcourt and Sprumont (Fig. 7C)
Calamospora sp.
Camarozonosporites ohioensis (Couper) Dettmann and Playford
Ceratosporites equalis Cookson and Dettmann (Fig. 7J)
Cyatheacidites annulatus Cookson (Fig. 7L)
Cyatheacidites archangelskii Dettmann (Fig. 7E)
Cyathidites australis/*C. minor* Couper
Densoisporites velatus Weyland and Krieger (Fig. 7G)
Dictyotosporites speciosus Cookson and Dettmann
Gleicheniidites senonicus Ross
Herkosporites sp.
Ischyosporites volkheimeri Filatoff (Fig. 7H)
cf. *Klukisporites scaberis* (Cookson and Dettmann) Dettmann
Laevigatosporites ovatus Wilson and Webster/*L. major* (Cookson) Krutzsch (Fig. 7K)
Lycopodiumsporites eminulus Dettmann
Peromonolites bowenii Couper (Fig. 7Q)
Perotrilites majus (Cookson and Dettmann) Evans (Fig. 7A)
Polypodiisporites favus (Potonié) Potonié
Polypodiisporites sp. (Fig. 7I)
Retitriletes austroclavatidites (Cookson) Döring et al. in Krutzsch (Fig. 7D)
Stereisporites antiquasporites (Wilson and Webster) Dettmann
Stereisporites regium (Drozhastichich) Drugg (Fig. 7F)
Todisporites major/*T. minor* Couper
Trilites parvallatus Krutzsch
Triporoletes radiatus (Dettmann) Playford (Fig. 7N)
Tuberculatosporites parvus Archangelsky

Pollen

Gymnosperm

Araucariacites australis Cookson (Fig. 7U)
Dacrycarpites australiensis Cookson and Pike
Dilwynites granulatus Harris (Fig. 7P)
Equisetosporites sp. (Fig. 7W)
Microcachrydites antarcticus Cookson ex Couper (Fig. 8A)
Phyllocladidites mawsonii Cookson ex Couper (Fig. 7V)
Podocarpidites major Couper (Fig. 7T)
Podocarpidites marwickii Couper
Podocarpidites otagoensis Couper (Fig. 7M)
Podocarpidites rugulatus Pocknall and Mildenhall (Fig. 7O, S)
Podocarpidites verrucosus Volkheimer
Podocarpidites spp.
Trichotomosulcites subgranulatus Couper (Fig. 8O)

Angiosperm

Battenipollis sectilis (Stover) Jarzen and Dettmann (Fig. 8B)
Ericipites scabratus Harris (Fig. 8K)
Liliacidites spp. (Fig. 8I)
Longapertites sp. Povilauskas et al. (Fig. 7R)
Monosulcites palisadus Couper
Monosulcites/*Arecipites* spp.
Myricipites harrisii (Couper) Dutta and Sah (Fig. 8G)
Nothofagidites americanus Zamaloa (Fig. 8J)
Nothofagidites dorotensis Romero
Nothofagidites saraensis Menéndez and Caccavari de Fílice (Fig. 8P)
Nothofagidites tehuelchesii Zamaloa and Barreda
Nothofagidites spp.
Peninsulapollis askiniae Dettmann and Jarzen (Fig. 8H)
Peninsulapollis gillii (Cookson) Dettmann and Jarzen (Fig. 8F)
Periporopollenites polyoratus (Couper) Stover in Stover and Partridge (Fig. 8L)
Proteacidites parvus Cookson (Fig. 8N)
Proteacidites scaboratus Couper (Fig. 8C)
Proteacidites tenuiexinus Stover in Stover and Partridge (Fig. 8E)
Proteacidites spp.
Tricolpites confessus Stover in Stover and Partridge (Fig. 8D)
Triorites orbiculatus McIntyre (Fig. 8M)

Dinoflagellate

Alterbidinium acutulum (Wilson) Lentin and Williams emend. Khowaja-Ateequzzaman, Garg and Jain (Fig. 9P)
Amphidiadema nucula (Cookson and Eisenack) Lentin and Williams (Fig. 9G)
Andalusiella mauthei Riëgel
Batiacasphaera grandis Roncaglia et al. (Fig. 10K, L)
Batiacasphaera rifensis Slimani et al. (Fig. 9A)
Batiacasphaera rugulata Schiøler and Wilson (Fig. 10H)
Batiacasphaera? reticulata (Davey) Davey (Fig. 9C, D)
Canningia sp. 1 in Schiøler and Wilson (Fig. 10G)
Canninginopsis bretonica Marshall (Fig. 9Y)
Canninginopsis ordospinosa Smith (Fig. 9BB)
Cerodinium ("*Ceratiopsis*") sp. in Mehrotra and Sarjeant (1987)
Chatangiella granulifera/verrucosa (Manum) Lentin and Williams (Fig. 9J)
Chatangiella victoriensis (Cookson and Manum) Lentin and Williams
Circulodinium distinctum (Deflandre and Cookson) Jansonius
Cyclonephelium compactum Deflandre and Cookson
Diconodinium cristatum Cookson and Eisenack emend Morgan
Diconodinium sp. cf. *multispinum* (Deflandre and Cookson) Eisenak and Cookson emend Morgan
Eurydinium ellipticum Mao and Mohr (Fig. 9M)
Impagidinium cristatum (May) Lentin and Williams (Fig. 10E, F)
Isabellidinium cooksoniae (Alberti) Lentin and Williams
Isabellidinium cretaceum (Cookson) Lentin and Williams (Fig. 9A)
Isabelidinium cretaceum gravidum Mao and Mohr (Fig. 9B)
Isabellidinium cretaceum oviforme Mao and Mohr (Fig. 9C)
Isabelidinium pellucidum (Deflandre and Cookson) Lentin and Williams (Fig. 9E, Fig. 11P, Q)
Isabellidinium papillum Sumner
Isabellidinium sp.
Kallosphaeridium parvum Jan du Chêne (Fig. 11C)
Kallosphaeridium? ringnesorium in Mohr and Mao (Fig. 11D)
Maduradinium pentagonum Cookson and Eisenack (Fig. 9K)
Manumiella conorata (Stover) Bujak and Davies (Fig. 9O)
Manumiella druggii (Stover) Bujak and Davies (Fig. 9N)
Manumiella seelandica (Lange) Bujak and Davies (Fig. 9R, T)
Manumiella seymourensis Askin (Fig. 9W, X)
Manumiella sp. cf. *M. bertodano* Thorn et al. (Fig. 9Z, AA)
Manumiella spp.
Membranilarnacia densa Cookson and Eisenack (Fig. 11L)
Membranilarnacia spp.
Nelsoniella aceras Cookson and Eisenack (Fig. 9L)
Nelsoniella tuberculata Cookson and Eisenack
Odontochitina indigena Marshall (Fig. 10O)
Odontochitina porifera Cookson (Fig. 10N, R)
Operculodinium centrocarpum (Deflandre and Cookson) Wall (Fig. 11I)
Operculodinium flucturum Davey
Operculodinium radiculatum Smith (Fig. 11F)

Palaeocystodinium granulatum (Wilson) Lentin and Williams (Fig. 9CC)
Paleocystodinium golzowense Alberti
Paleocystodinium pilosum Guler et al. (Fig. 9I, Q)
Phelodinium exilicornutum Smith (Fig. 9U)
Pterodinium cretaceum Slimani et al. (Fig. 10I, J)
Saeptodinium gravattensis Harris (Fig. 9DD)
Senegalinium bicavatum Jain and Millepied (Fig. 9H)
Spinidium essoi Cookson and Eisenack (Fig. 9D)
Spiniferites pseudofurcatus (Klump) Sarjeant (Fig. 11E)
Spiniferites ramosus (*ramosus–multibrevis–granosus*) complex (*S. ramosus* (Ehrenberg) Mantell) (Fig. 11A, B, L, O)
Spongodinium reticulatum Hultberg (Fig. 10B)
Trichodinium castaneum (Deflandre) Clarke and Verdier – *T. chilensis* Troncoso and Doubinger, complex (Fig. 10M, P, Q)
Valensiella reticulata (Davey) Courtinat
Xenascus ceratioides (Deflandre) Davey and Verdier (Fig. 11G)
Xenascus plotei Below (Fig. 11H, J)
Xenikoon australis Cookson and Eisenack (Fig. 9F)

Chlorophyceae
Botryococcus brauni Kützing (Fig. 8Q)
Dictyotidium sp.
Leiosphaeridia sp.
Nummus monoculatus Morgan (Fig. 8R, U)
Palambages spp. (Fig. 8X)
Paralecaniella indentata (Deflandre and Cookson) Cookson and Eisenack emend Elsik (Fig. 8S)
Pterospermella australensis (Deflandre and Cookson) Eisenack
Pterospermella aureolata (Deflandre and Cookson) Eisenack (Fig. 8V)
Pterospermella spp.
Tetraedron cf. *minimum* (A. Braun) Hansgirg (Fig. 8T)
Acritarchs
Michrystridium piliferum Deflandre (Fig. 8W)
Fungi, Microthyriaceae
Asterothyrites Cookson (Fig. 8Y)
Organic foraminiferal linings (Fig. 8Z, AA)
Arthropod (Copepods) eggs (Fig. 11M)